American Mineralogist, Volume 74, pages 307–324, 1989

Geochemical evolution of the Maloin Ranch pluton, Laramie Anorthosite Complex, Wyoming: Petrology and mixing relations

ALLAN KOLKER, DONALD H. LINDSLEY
Department of Earth and Space Sciences, State University of New York, Stony Brook, New York 11794, U.S.A.

ABSTRACT

The Maloin Ranch pluton is a half-bowl–shaped composite intrusion containing a succession of rock types starting with ferrodiorite at the base, overlain progressively by fine-grained and porphyritic monzonite, monzosyenite, and, at the top, porphyritic granite. A progressive increase in Fe/(Fe + Mg) and corresponding alkali enrichment with height in the intrusion are shown by major-element analyses and by compositions of plagioclase, pyroxene, olivine, amphibole, and biotite. Maloin rock types and trends in mineral chemistry are similar to those in the Sybille Monzosyenite, to the northwest, which Fuhrman et al. (1988) have interpreted as a continuous fractionation series from monzogabbro (= ferrodiorite) to monzosyenite.

Emplacement temperatures were near 1000 °C for fine-grained monzonites and 900–950 °C for monzosyenites, as estimated from pyroxenes and by saturation thermometers. Pressures of 4.0–4.5 kbar are indicated for monzosyenites by the breakdown of Fe-rich pigeonite to fayalite + hedenbergite + quartz and by the Al content of coexisting amphibole. Magmatic f_{O_2} was controlled by the equilibrium quartz + ulvöspinel = ilmenite + fayalite (QUIIF; Frost et al., 1988a), with a primary f_{O_2} one to two log units below FMQ.

At least three contemporaneous magmas were present in the Maloin Ranch pluton. Fine-grained monzonite and biotite gabbro magmas repeatedly injected and covered the floor of a monzosyenite magma chamber, forming an ~250-m-thick layered zone in which all three rock types are conformably interlayered. Fine-grained monzonite and monzosyenite mixed locally and produced porphyritic monzonite, intermediate in texture and Fe enrichment. The porphyritic monzonites show that a portion of the ferrodiorite-monzosyenite suite in the Maloin Ranch pluton did *not* form by fractionation in a continuous series.

INTRODUCTION

The Maloin Ranch pluton is a stratified composite intrusion emplaced into anorthositic rocks at the southeast margin of the Laramie Anorthosite Complex (Fig. 1). The pluton includes ferrodiorite, ferromonzonite, monzosyenite, and granite, an assemblage that is present at the margins of Proterozoic anorthosites throughout the world (e.g., Morse, 1982; Duchesne, 1984; Emslie, 1985). The origin of large granitic bodies surrounding anorthosite massifs can be attributed to crustal anatexis, based on trace-element, isotopic, and volumetric considerations (Ashwal and Siefert, 1980; Emslie, 1980; Duchesne et al., 1985a). The origin of the ferrodiorite-ferrosyenite portion of the assemblage has evoked considerable debate, centered on the relative importance of (1) fractionation of residual liquids from the anorthosite parent magma(s) (e.g., Philpotts, 1966; Morse, 1982) versus (2) partial melting of the lower crust (Ashwal and Siefert, 1980; Duchesne et al., 1985b) or upper crust (Buddington, 1972). For the Laramie Complex, Fountain et al. (1981) considered the syenitic rocks to be the product of crustal anatexis, on the basis of trace-element and isotopic data. Alternatively, Fuhrman et al. (1988) have shown a continuous gradation in mineral compositions between the Laramie Anorthosite and the Sybille Monzosyenite and have suggested a possible comagmatic relationship.

This paper constitutes the first portion of an integrated field, petrologic, and geochemical study, with the primary purpose of determining the origin of the ferrodiorite to granite suite at the southeast margin of the Laramie Anorthosite. The objective of this paper is to present petrologic data with which geochemical models can be later developed. A subsidiary goal of this paper is to compare crystallization conditions in the Maloin Ranch pluton with those in the Sybille Monzosyenite and in similar intrusions. The Maloin Ranch pluton provides a good opportunity to investigate magmatic processes at anorthosite margins because the characteristic range in rock types is present in the well-exposed stratigraphic succession. Previous work in the study area is limited to reconnaissance mapping (Fowler, 1930; Newhouse and Hagner, 1957) and several Sr-isotope analyses (Subbarayudu, 1975).

The Laramie Anorthosite Complex is exposed over an area of about 1000 km² in southeastern Wyoming (Fig. 1). The complex was emplaced across the Cheyenne belt,

0003–004X/89/0304–0307$02.00

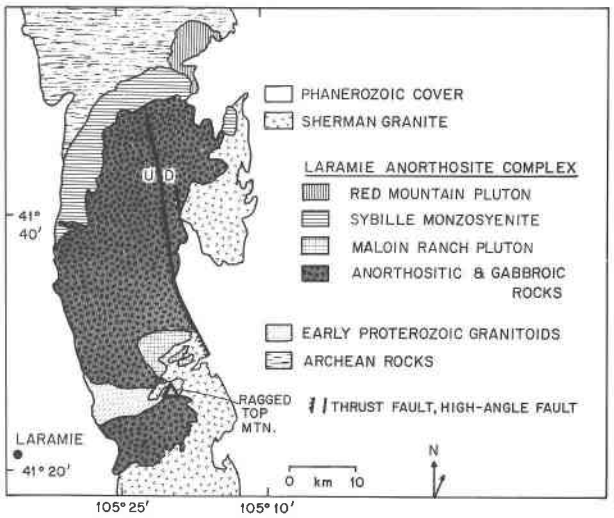

Fig. 1. Generalized geologic map of the Laramie Anorthosite Complex. Major monzonitic and syenitic intrusions include Sybille Monzosyenite (to the northwest), Red Mountain pluton (to the north), and the Maloin Ranch pluton (to the southeast). Modified from Newhouse and Hagner (1957).

a major discontinuity separating Archean basement in the Wyoming province to the north from early Proterozoic basement to the south (Karlstrom and Houston, 1984; Deubendorfer and Houston, 1987; Geist et al., 1987; Kolker et al., 1987). In the northern part of the complex, anorthosite and associated rocks intrude Archean granitic gneisses and associated supracrustal rocks (Fowler, 1930; Newhouse and Hagner, 1957; Klugman, 1966; Hills and Armstrong, 1974; Snyder, 1984). To the south and east, the Laramie Complex is bounded by the Sherman Granite, a regionally extensive anorogenic intrusive.

The age of the anorthosite (~1430 Ma) is inferred from U-Pb dating of concordant zircons in adjacent rocks that intrude it. These include monzosyenites (1430 ± 15 Ma; Subbarayudu et al., 1975), the Sherman Granite (1430 ± 20 Ma; Subbarayudu et al., 1975; Aleinikoff, 1983; R. E. Zartman, pers. comm., 1987), and the Red Mountain pluton (1440 ± 6 Ma; Frost et al., 1988b), which intrudes the Sybille Monzosyenite. The zircon data are consistent with field relations suggesting that the major members of the Laramie Anorthosite Complex and the Sherman Granite were intruded in rapid succession.

Field relations

Structure and stratigraphy

The Maloin Ranch pluton is an open bowl–shaped body exposed over an area of about 50 km² (Fig. 2). The pluton is truncated to the east by Laramide faulting and grades into porphyritic granites of Sherman Granite affinity to the southeast. Southwest of the pluton, a septum of early Proterozoic(?) granitoids, pelitic gneiss, and granulite forms the southern margin of the main anorthosite mass.

Unlike the Sybille Monzosyenite, the Maloin Ranch pluton has a well-defined stratigraphy (Fig. 3). Ferrodiorite (FDi) occupies the lowest part of the pluton, adjacent to the anorthosite contact, and is overlain progressively by (1) fine-grained monzonite (FMZ) and porphyritic monzonite (PMZ), (2) monzosyenite (MSY), and (3) porphyritic granite.

Within the lower (FDi to PMZ) portion of the pluton, layering is defined by concentration and local alignment of scattered feldspar megacysts and by the attitude of alternating fine-grained and porphyritic zones. The strike of the layers parallels the anorthosite contact and dips inward, away from the anorthosite, at 20° to about 45°. There is no apparent flattening of dips away from the anorthosite contact. Although few attitudes could be taken on the massive monzosyenite portion of the pluton, localized indistinct layering also dips away from the anorthosite, suggesting that the structure may be open to the southeast or perhaps truncated by the Sherman Granite.

Rock types and petrography

Ferrodiorite-fine-grained monzonite series. Ferrodiorite (FDi) occurs primarily along the basal contact with anorthositic rocks, extending only 100–200 m away from the contact (Fig. 2). Small bodies of FDi are also present locally within anorthosite near the contact. The Maloin FDi is similar in occurrence to oxide-rich monzogabbro at the eastern margin of the Sybille Monzosyenite (Fuhrman et al., 1988), and its bulk composition is similar to that of Fe-Ti-P_2O_5–enriched diorites thought to be anorthosite residua (i.e., Wiebe, 1980a; Emslie, 1980; Ashwal, 1982). The Maloin FDi is typically fine- to medium-grained and consists of plagioclase, augite, low-Ca pyroxene (inverted pigeonite?), composite ilmenite-titanomagnetite, and apatite (Table 1). Augite is less abundant than low-Ca pyroxene. Away from the anorthosite contact, FDi grades upward into fine-grained monzonite by a progressive increase in alkali feldspar and modest corresponding decreases in total pyroxene, Fe-Ti oxides, and apatite (Table 1).

Fine-grained monzonite (FMZ; "norite" of Newhouse and Hagner, 1957) forms most of the lower portion of the pluton (Figs. 2 and 3). FMZ is generally finer grained than adjacent FDi, but grades locally into medium-grained equivalents (e.g., GM 25). The FMZ contains two pyroxenes—ferroaugite and inverted pigeonite—and two feldspars—plagioclase and microperthite (Table 1). Unlike in the Sybille body, textural evidence of ternary feldspars has not been found in Maloin FDI and FMZ. Zircon is absent from the FDi and uncommon in FMZ, as neither magma was saturated in this phase at high temperature (see Geothermometry).

Biotite gabbro. Biotite gabbro occurs locally as minor conformable and/or crosscutting bodies resembling FDi and FMZ in outcrop. Biotite gabbro consists largely of intermediate plagioclase, two pyroxenes, evenly distributed red-brown biotite, and composite ilmenite-magnetite. Olivine and brown hornblende are present in some

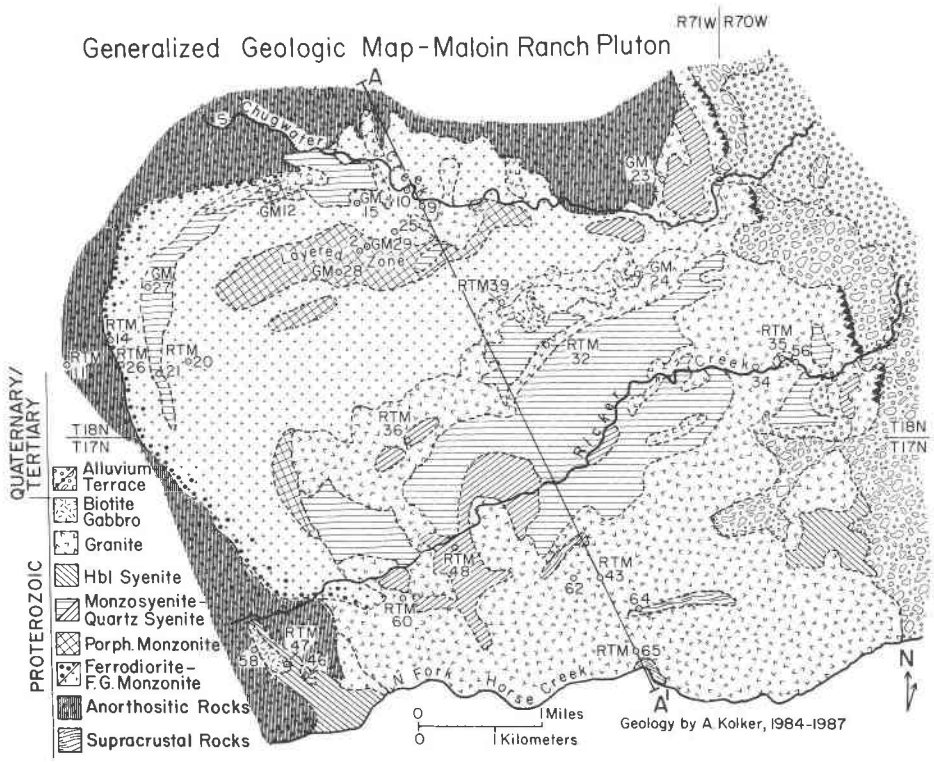

Fig. 2. Generalized geologic map of the Maloin Ranch pluton showing location of representative samples, layered zone, and line of cross section A–A′ (see Fig. 3). See Kolker (1989) for additional sample locations and petrographic descriptions. Sawteeth show distribution of exposed fault gouge along the east-bounding Laramide thrust fault. Quaternary-Tertiary terrace deposits cover upturned Paleozoic-Mesozoic rocks (not shown) at the eastern margin of the map area.

samples. In the finest-grained (chilled) samples, lathlike plagioclase is present in subophitic intergrowths.

Monzosyenite. Monzosyenite (MSY) occupies a large portion of the Maloin pluton, stratigraphically upward from the FMZ. Monzosyenite is used here for coarse-grained two-feldspar cumulates that have been called monzonite (Fountain et al., 1981) or syenite (Klugman, 1966; and others). The name monzosyenite was used by Lindsley et al. (1985) and Fuhrman et al. (1988) for equivalent rocks in the Sybille body that contain ternary feldspar. Although ternary feldspar is lacking in the Maloin Ranch pluton, monzosyenite is retained for consistency and because of the likelihood that ternary feldspar was present prior to subsolidus re-equilibration.

Maloin MSY is characterized by subequant, interlocking megacrysts of 1- to 3-cm perthite (and less commonly, plagioclase), in a matrix dominated by ferromagnesian minerals, plagioclase, and varying amounts of quartz. Myrmekite is very common in albitic plagioclase concentrated at the margins of alkali feldspar megacrysts. Some perthite megacrysts are partially replaced by microcline, possibly indicating late influx of water (Parsons and Brown, 1984). Ferromagnesian minerals in the MSY include ferroaugite, inverted pigeonite, and fayalite. These minerals are largely concentrated in clots, which are locally enclosed by green ferrohornblende, and less commonly, by grunerite. Ilmenite, abundant zircon, and scattered euhedral apatite are common minor constituents (Table 1). MSY grades upward into quartz syenite (QSY) and porphyritic granite, with little change in grain size or

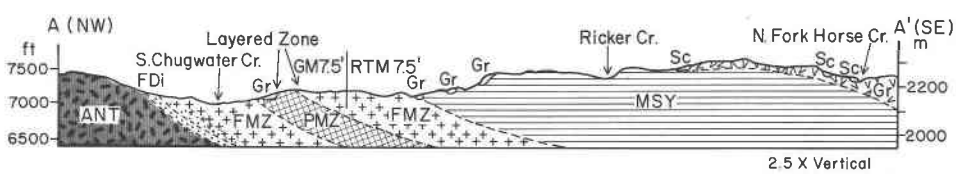

Fig. 3. Northwest to southeast cross section through the Maloin Ranch pluton along line A–A′ (see Fig. 2). Patterns are the same as in Fig. 2. Unpatterned areas are granitoid dikes (Gr) and supracrustal inclusions (Sc). Vertical exaggeration is 2.5 times actual topography.

texture. Mafic clots resembling those in Maloin MSY have been observed in a Quebec quartz mangerite, interpreted by Philpotts (1981) as segregations of immiscible Fe-rich melt. Although this process cannot be excluded for mafic clots in MSY, trace-element data suggest that the associated FDi and FMZ are not related to MSY by immiscibility (Kolker, 1989).

Porphyritic monzonite. Contacts between fine-grained monzonite and coarse monzosyenite are generally sharp. Porphyritic monzonite (PMZ), present locally, appears to be the result of mixing between FMZ and MSY. The PMZ texture is characterized by scattered megacrysts of alkali feldspar and clots of clinopyroxene or inverted pigeonite, in a fine-grained monzonitic matrix (Fig. 4). Within these mixed rocks, zircon is concentrated near, or intergrown with the pyroxene clots, strongly suggesting that it was contributed by the zircon-saturated MSY (Fig. 5). Their intergrowth with abundant zircon indicates that the pyroxene clots are not remobilized fragments of coarser FMZ. The high Zr content of FMZ sample GM 9 (603 ppm) compared to that of GM 15 A (near average at 363 ppm) can be attributed to inclusion of zircon xenocrysts, as shown in Figure 5. Most of the area mapped as PMZ includes a zone of interlayered FMZ, biotite gabbro, PMZ, and MSY (see the section on the layered zone).

Granites. Several distinct varieties of granite were recognized in the Maloin Ranch pluton. Some coarse-grained porphyritic granite is found only near bodies of MSY and QSY, in a transitional series (e.g., south and east of RTM 48; Fig. 2). In this vicinity, orange-weathering MSY and QSY are exposed in drainages, whereas pink-weathering porphyritic granite is exposed on surrounding ridges. The upward transition is marked by (1) decreasing content of ferromagnesian minerals, (2) replacement of pyroxene and olivine with ferrohornblende and biotite, (3) replacement of perthitic orthoclase by microcline-perthite, and (4) increasing quartz (Table 1). Similar trends have been observed in the zoned Kleivan granite of southwest Norway (Petersen, 1980) and in some Nain adamellites (Wheeler, 1969), but these granitic bodies also contain ternary mesoperthite. Myrmekite, a characteristic of the syenitic rocks, is present throughout the MSY to granite transition.

Away from bodies of MSY and QSY, the coarse-grained porphyritic granite grades into a medium-grained porphyritic granite having subequant feldspar megacrysts (e.g., RTM 62). The medium-grained granite occupies the uppermost portion of the Maloin pluton and locally contains abundant inclusions of supracrustal country rocks. We interpret the medium-grained granite as a melt envelope at the outer (upper) margin of the Maloin Ranch pluton. Minerals of the medium-grained granite are similar to those of the coarse-grained porphyritic granite, but the former entirely lacks orthoclase and pyroxene and contains more than 35 modal percent quartz.

Farther south and east (e.g., RTM 65), the medium-grained granite grades into coarse-grained porphyritic granite, which resembles portions of the Sherman Granite in its grain size (up to ~4 cm) and presence of tabular, zoned microcline. Much of the southeast corner of the map area is composed of this Sherman-like granite, consistent with indications from reconnaissance mapping that the "southeastern syenite" grades into the Sherman body (Newhouse and Hagner, 1957).

TABLE 1. Modal minerals in the Maloin Ranch pluton

	Ferrodiorite		Fine monzonite			Monzosyenite		Quartz syenite		Porphyritic granite	
Sample:	RTM 14	RTM 26	GM 9	GM 15A	GM 25	GM 27	RTM 35	RTM 36	RTM 48	RTM 56	RTM 39
Alkali feldspar*	—	—	15.0	13.5	12.1	63.4	54.7	52.2	52.4	44.6	43.8
Plagioclase	49.2	46.4	44.3	46.2	43.6	25.7	25.1	29.6	19.3	18.4	16.8
Quartz**	—	—	—	—	—	3.6	8.5	15.0	16.9	33.6	34.7
Orthopyroxene (inverted pigeonite?)	27.6	27.4	18.0	17.7	22.4	4.8	3.9	—	—	—	—
Clinopyroxene	7.3	9.9	11.1	7.1	6.7	0.6	2.0	0.1	2.0	—	—
Olivine†	—	—	—	2.5	1.7	—	1.2	0.7	1.7	—	—
Hornblende	—	—	—	0.2	—	0.8	1.9	1.9	3.7	0.8	0.5
Biotite	0.2	0.2	2.4	1.3	3.0	0.1	tr	0.1	1.5	2.5	3.9
Ilmenite	6.6	5.9	4.3	4.8	5.1	0.6	2.0	0.3	1.0	tr	0.3
Magnetite††	5.0	5.4	2.3	3.1	1.6	0.1	0.1	tr	tr	tr	tr
Apatite	4.1	4.8	2.4	3.6	3.8	0.3	0.3	0.1	0.4	0.1	tr
Total	100.0	100.0	99.8	100.0	100.0	100.0	99.7	100.0	99.2	100.0	100.0
Accessory minerals											
Zircon	—	—	tr	tr	—	tr	0.3	tr	0.1	tr	tr
Sphene	—	—	—	—	—	—	—	—	—	—	tr
Grunerite	—	—	—	—	—	—	—	—	0.7	—	—
Epidote	—	—	—	—	—	—	—	—	—	—	—
Sulfide	—	—	0.2	tr	tr	tr	tr	—	tr	—	—
Other	tr‡	tr‡	—	—	—	—	—	—	—	—	—

Note: Dash (—) means not observed; tr means present, but not observed in point counts.
* Perthite in FMZ-MSY; microcline in granites; both in QSY.
** Includes some quartz in myrmekite.
† Includes some alteration products.

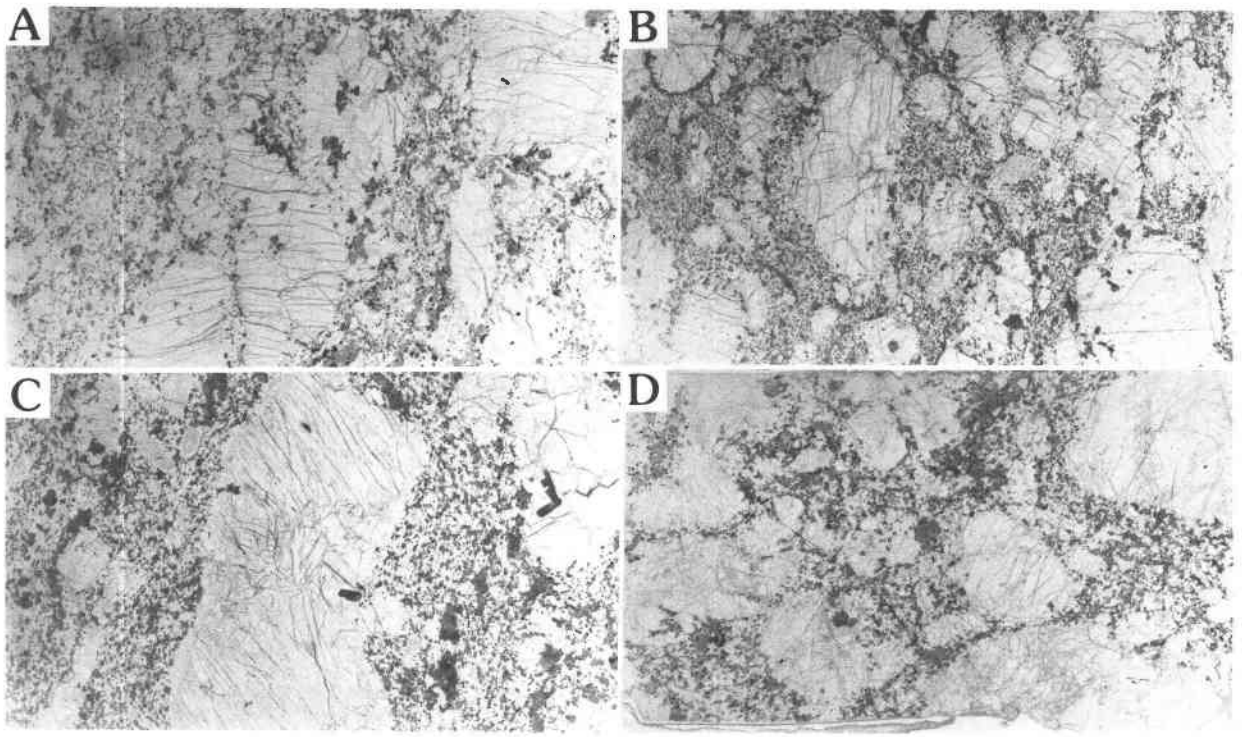

Fig. 4. Textures of porphyritic monzonites resulting from mixture of fine monzonite and monzosyenite in the layered zone. Photos are entire thin sections (width of field of view = 40 mm). Each section shows megacrysts of alkali feldspar and pyroxene clots contributed by the MSY, with patches of the FMZ matrix. **(A)** Sample GM 29C. **(B)** Sample GM 2M. **(C)** GM 2A. **(D)** GM 10B.

TABLE 1.—*Continued*

Porphyritic granite		Granitic dikes		Biotite gabbro	
RTM 62	RTM 65	GM 23	RTM 32	RTM 46	GM 24
42.3	45.8	25.9	47.9	—	—
18.4	17.0	39.8	19.3	58.5	61.3
36.8	29.1	22.1	32.1	—	—
—	—	—	—	11.6	12.7
—	—	—	—	3.3	8.7
—	—	—	—	8.6	7.3
1.2	4.8	0.6	—	7.1	2.9
0.7	1.2	11.0	0.5	9.0	6.7
0.1	0.4	tr	—	1.6	0.2
0.5	1.1	tr	0.2	—	0.2
tr	tr	0.3	—	0.3	tr
100.0	99.4	99.7	100.0	100.0	100.0
		Accessory minerals			
tr	tr	0.1	—	—	—
—	tr	0.2	—	—	—
—	tr	—	—	—	—
tr	—	tr	—	—	—
—	—	—	—	tr	tr
—	0.6§	—	—	—	—

†† Includes hematite after magnetite.
‡ Goethite.
§ Alteration after pyroxene (?).

Dikes and small intrusive bodies of fine-grained granitoids crosscut all units in the Maloin pluton and the surrounding anorthositic rocks. Mafic mineral content in the fine-grained granites varies from near zero in some aplitic dikes (e.g., RTM 32), to about 10 percent (e.g., GM 23; Table 1).

Layered zone. The most distinct igneous layering in the Maloin Ranch pluton is exposed between GM 28 and GM 10 (Fig. 2), where layers of MSY ranging in thickness from a few centimeters to several meters are conformably interlayered with FMZ and/or biotite gabbro (Fig. 6). This layered zone dips away from the anorthosite at 25° to 30° and has a thickness of about 250 m. The sequence of layering is shown in two measured sections (Fig. 7). Thick (>5 m) layers consisting largely of biotite gabbro are present near the base of each section. At their margins, both FMZ and biotite gabbro are distinctly chilled against underlying and, less commonly, overlying MSY layers. The grain size of the thicker layers of FMZ and biotite gabbro coarsens progressively toward their centers. The fine-grained margins of these layers are locally disrupted by penetration of overlying MSY alkali feldspar megacrysts, suggesting that the magmas that formed these layers were not entirely solidified when the overlying cumulates were emplaced.

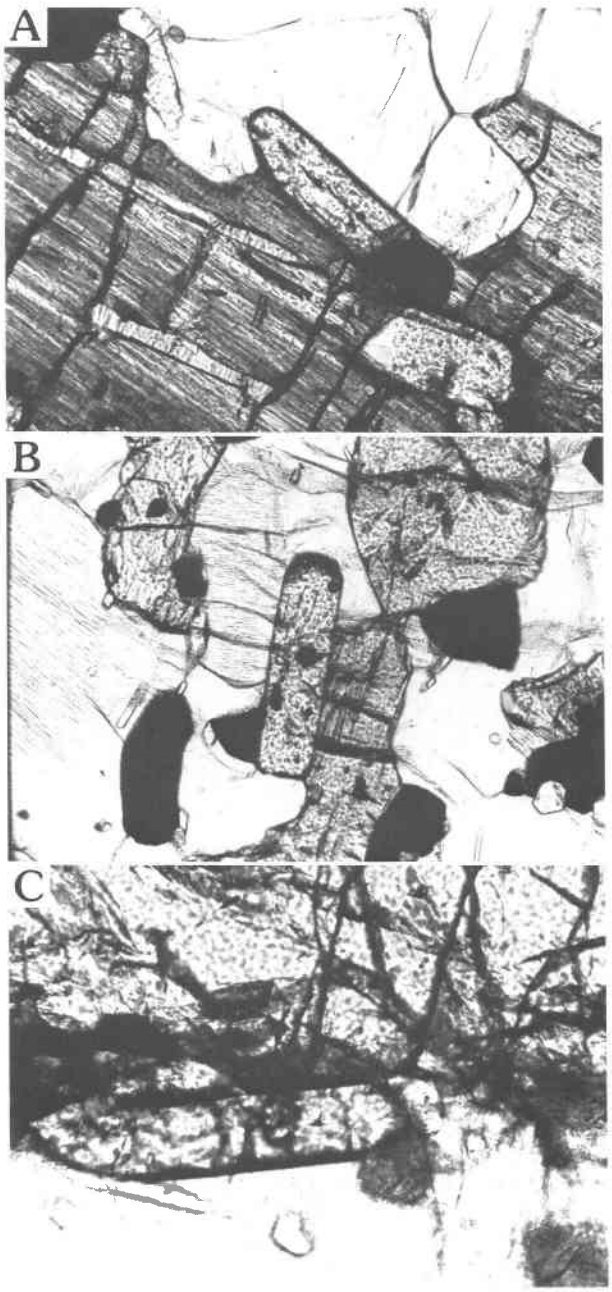

Fig. 5. Pyroxene aggregates poikilitically enclosing zircon. **(A)** Monzosyenite, sample GM 27. **(B)** Porphyritic monzonite, sample GM 29C. **(C)** Fine-grained monzonite, sample GM 9. Width of field for all photomicrographs is 0.95 mm. In (B) and (C), zircon is only present within or adjacent to pyroxene clots, not in FMZ matrix.

The features described above are remarkably similar to relations between fine-grained gabbro and cumulate diorite at Ingonish, Cape Breton Island, described by Wiebe (1974a, 1974b). Borrowing from his model, we suggest that the layers of FMZ and biotite gabbro were chilled at their margins upon injection into an MSY magma chamber that was cooler by perhaps 100 °C. As they were injected, these magmas spread and covered the floor of the host chamber. As the "flows" cooled, cumulus alkali feldspar would nucleate on the chilled surface, forming an intervening MSY layer (compare Wiebe, 1974a, Fig. 17). Scouring, or injection of subsequent fine-grained layers would truncate some chilled margins.

Another characteristic of the layered zone is the presence of black plagioclase, identical to that in nearby anorthositic rocks, as xenocrysts in FMZ, MSY, and biotite gabbro. The dark xenocrysts have $\sim An_{50}$ cores with oriented inclusions of ilmenite(?), rimmed by inclusion-free plagioclase ($\sim An_{30}$), showing disequilibrium. The xenocrysts typically occur as <1-cm crystal fragments, but at GM 2 and GM 10, 1- to 2-m-thick layers of euhedral, 2- to 5-cm black plagioclase are present in biotite gabbro. The biotite gabbro magma appears to have passed through anorthositic crystal mush prior to emplacement in the Maloin pluton, with suspended plagioclase xenocrysts becoming concentrated by flow differentiation. The presence of black plagioclase in the FMZ suggests that it used the same pathway(s) as the biotite gabbro to inject the MSY cumulates. Locally, mixing has produced complex hybrids between four end-members—biotite gabbro, plagioclase xenocrysts, alkali feldspar cumulates, and fine-grained monzonite (GM-2 series; Fig. 4). The limited extent of the layered zone (~ 3 km^2) may reflect proximity to feeder pipes for the FMZ and biotite gabbro magmas, although such pipes were not observed.

Major elements

Major-element compositions of a suite of whole-rock samples from the Maloin Ranch pluton were determined by X-ray fluorescence on fused-glass discs (Norrish and Hutton, 1969), at the University of Massachusetts, Amherst. Prior to fusion, rock powders were dried in air at 1000 °C for 2 h, driving off volatiles and oxidizing all Fe to Fe^{3+}. Analyses given in Table 2 are anhydrous compositions normalized to the original (Fe^{3+}) totals, after recalculation of Fe to Fe^{2+}.

The most pronounced major-element characteristics of the FDi to MSY series are progressive increases in SiO_2, Al_2O_3, and alkalis with relative Fe enrichment, and corresponding decreases in CaO, FeO_t, MgO, TiO_2, and P_2O_5 (Table 2). Major-element data for the FDi to MSY series in Maloin and Sybille are plotted versus cation fraction $Fe_t(Fe_t + Mg)$, in Figure 8. For most oxides, values for FMZ and PMZ are intermediate to those for FDi and MSY. MSY is silica oversaturated with 5–6% CIPW-normative quartz (calculated with all Fe as FeO) at an average SiO_2 content of 62 wt% (Table 2; Fig. 8). In FDi, FMZ, and MSY, predominance of Opx over Cpx is also reflected in the norms, in contrast to Sybille, in which normative Opx (Fountain et al., 1981) is expressed modally as fayalite + quartz (Fuhrman et al., 1988). The oxide plots show that for a given rock type, Maloin is less Fe-enriched than Sybille, suggesting that the two intrusions evolved along analogous but not identical paths.

Fig. 6. Layered zone, showing conformable alternation of fine-grained layers consisting of FMZ and/or biotite gabbro (darker bands), with alkali feldspar cumulates (lighter bands). Width of view is about 3 m.

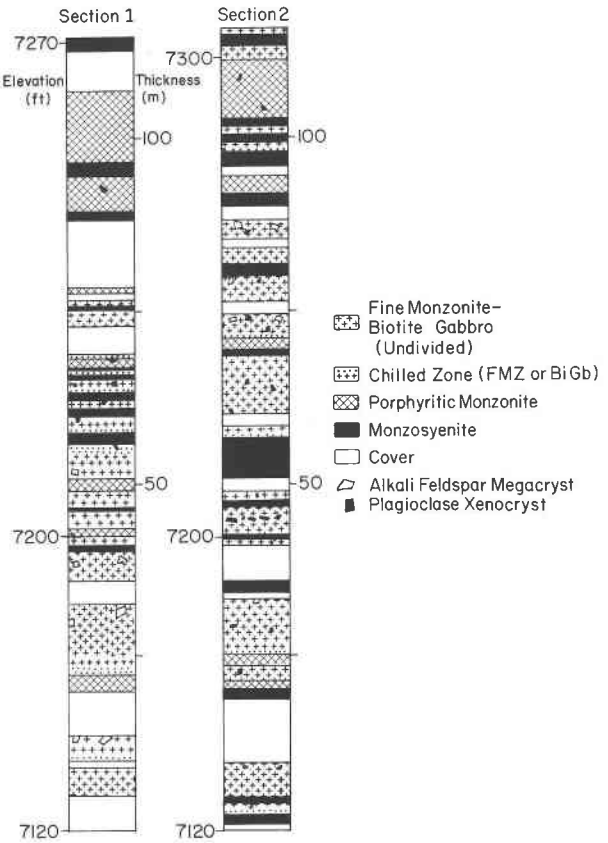

Fig. 7. Stratigraphic sections of a portion of the layered zone showing lithologic variation, location of prominent FMZ and biotite gabbro chill zones, and distribution of anorthositic plagioclase xenocrysts. Sections were measured about 0.7 km apart, between GM 2 (=section 2) and GM 25 (near section 1). Symbols are modified from Fig. 2.

$Fe_t/(Fe_t + Mg)$ ratios for biotite gabbro range from 0.4 to 0.5, considerably lower than those for Maloin FDi. A porphyritic granite and several granitic dikes have very high SiO_2 contents and are mildly peraluminous.

Major-element data plotted versus $Fe_t/(Fe_t + Mg)$ for a Maloin porphyritic monzonite (GM 12F) are inconsistent with either mixing of FMZ and MSY or fractional crystallization of FMZ liquid (Fig. 8). The low $Fe_t/(Fe_t + Mg)$, TiO_2, FeO_t, and P_2O_5 contents of this sample compared to other (Sybille) PMZ, suggest that Fe-Ti oxides and apatite have been removed.

Mineral chemistry

Mineral compositions were determined with the Cameca Camebax electron microprobe at SUNY–Stony Brook, using an accelerating potential of 15 kV and beam currents ranging from 20 to 35 nA. Except for compositions of lamellae, all analyses were done in the raster mode, with a spot size of ~65 μm^2 for routine work and a larger spot (~250 μm^2) for feldspars and integration of exsolved grains. The raw data were processed using a ZAF correction procedure. Pyroxenes were integrated using a minimum of 35 analyses per grain, giving at least 50% of complete coverage along 3–4 traverse lines per grain, with traverses spaced at intervals of about 25 μm. Feldspar and pyroxene analyses for about 15 samples were obtained at Stony Brook using the ARL-EMX microprobe, with an acceleration potential of 15 kV, a sample current of 15 nA on brass, and the data-reduction procedure of Bence and Albee (1968).

Pyroxenes and olivines

The progressive Fe-enrichment of the Maloin Ranch pluton is well illustrated by the composition of pyroxenes in rocks ranging from biotite gabbro to granite (Fig. 9). The large range in Wo content for a given sample in Figure 9 is attributed to fine-scale lamellar and granule exsolution, as shown by Livi (1987) for a Sybille FMZ. Representative pyroxene compositions are given in Table 3. Maloin pyroxenes show no enrichment in Na with progressive Fe enrichment.

Pyroxenes in the layered zone show the alternation of mafic magmas that have injected the cumulate host (Fig. 10). In samples showing textural evidence of mixing, the composition of coarse pyroxene inclusions is remarkably similar to that of FMZ host pyroxenes, suggesting that re-equilibration has been extensive. Mixing has produced a few samples with unusually large ranges in Fe/(Fe + Mg) (e.g., Opx in GM 29). There is no apparent trend to the stratigraphic variation in composition (Fig. 10).

Olivines show the largest range in Fe/(Fe + Mg) ratios in the pluton (Fig. 9). The trend is less continuous than that of pyroxene because olivine is not present in all rock types. The most Fe-enriched compositions are in the MSY and QSY (Fa_{93}–Fa_{97}; Table 4). MnO is the most significant minor constituent in olivine, increasing progressively from about 1.0% in FMZ to 1.5% in the QSY.

TABLE 2. Major-element analyses from rocks of the Maloin Ranch pluton

	Anorthosite			FDi	FMZ		PMZ	MSY			Biotite gabbro	
	RTM 11A	RTM 58	BM 4A	RTM 26	GM 9	GM 15A	GM 12F	GM 12G	GM 27	RTM 35	GM 24	RTM 34B
SiO_2	53.93	53.81	50.80	44.78	50.41	49.83	55.97	61.80	62.06	62.75	49.83	47.69
TiO_2	0.26	0.39	0.69	4.43	3.18	2.95	1.57	0.72	0.65	0.73	0.96	1.40
Al_2O_3	27.60	27.29	20.43	14.06	14.27	14.10	15.39	17.95	17.35	16.81	17.97	17.67
FeO(t)**	1.62	1.66	9.48	16.69	14.25	15.31	12.01	5.53	4.89	5.70	10.19	10.85
MnO	0.02	0.02	0.13	0.26	0.22	0.25	0.22	0.10	0.09	0.10	0.15	0.23
MgO	0.36	0.44	6.05	5.33	3.27	2.92	2.87	0.42	0.51	0.50	8.84	7.71
CaO	10.93	11.09	8.37	9.89	7.61	7.33	5.69	3.56	2.64	2.88	8.24	10.65
Na_2O	4.50	4.45	3.45	2.57	3.47	3.33	3.86	4.76	4.19	4.29	2.74	1.82
K_2O	0.63	0.77	0.68	0.40	2.17	2.33	2.7	4.43	6.28	5.61	0.83	2.14
P_2O_5	0.09	0.11	0.15	2.01	1.25	1.48	0.16	0.18	0.20	0.16	0.16	0.17
Total	99.94	100.03	100.23	100.42	100.10	99.83	100.44	99.45	98.86	99.53	99.95	100.33
CIPW norms based on all Fe as FeO												
Q	0.54	0.20	0.00	0.00	0.00	0.00	0.38	5.66	4.51	6.25	0.00	0.00
C	0.00	0.00	0.00	0.00	0.00	0.00	0.00	0.00	0.00	0.00	0.00	0.00
or	3.72	4.55	4.02	2.36	12.82	13.77	15.96	26.18	37.11	33.15	4.91	12.65
ab	38.08	37.66	29.19	21.75	29.36	28.18	32.66	40.28	35.45	36.30	23.19	12.48
an	53.25	52.22	38.25	25.65	16.95	16.65	16.69	14.53	9.99	10.04	34.28	33.73
ne	0.00	0.00	0.00	0.00	0.00	0.00	0.00	0.00	0.00	0.00	0.00	1.58
di	0.33	1.77	1.90	8.68	10.79	8.64	8.97	1.71	1.57	2.80	4.72	14.86
hy	3.31	2.64	9.91	17.74	12.97	14.40	22.43	9.30	8.52	9.23	13.05	0.00
ol	0.00	0.00	15.30	11.18	8.26	9.17	0.00	0.00	0.00	0.00	17.61	21.98
il	0.49	0.74	1.31	8.41	6.04	5.60	2.98	1.37	1.23	1.39	1.82	2.66
ap	0.21	0.25	0.35	4.66	2.90	3.43	0.37	0.42	0.46	0.37	0.37	0.39

* From shear zone.
** Total Fe as FeO.

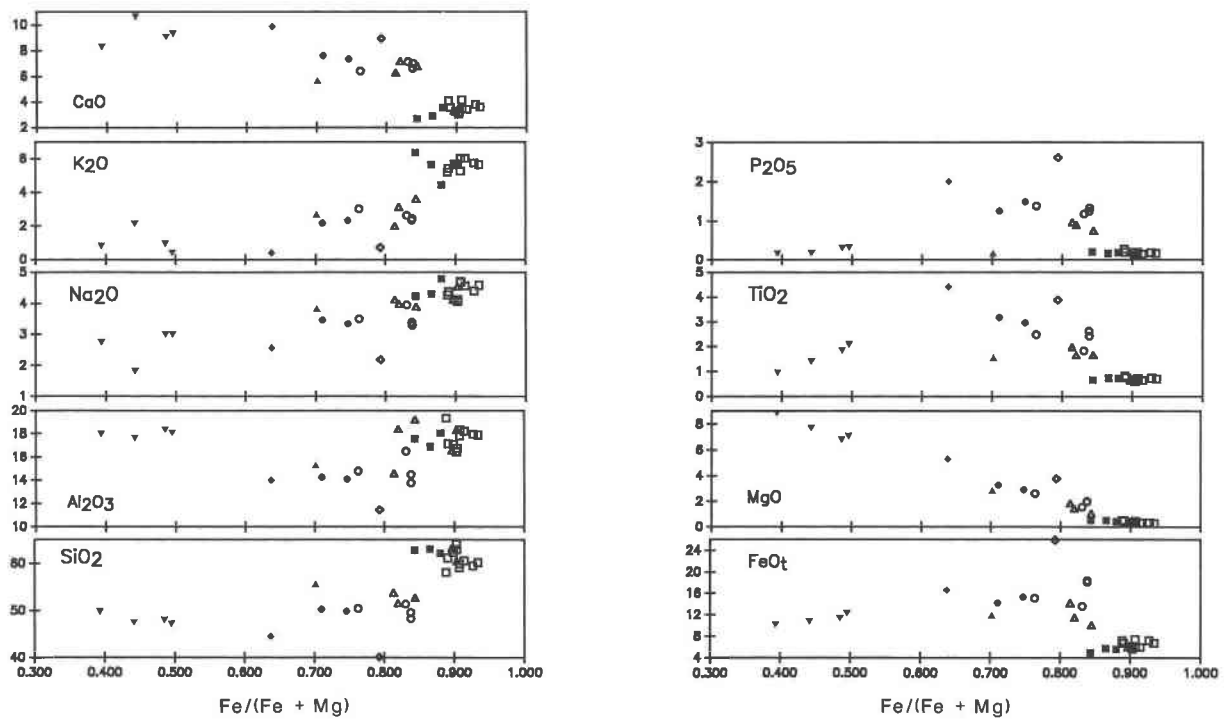

Fig. 8. Major-element data for the Maloin Ranch pluton (solid symbols) and Sybille Monzosyenite (open symbols). Oxides are plotted in weight percent vs. Fe enrichment, expressed as the cation fraction $Fe_t/(Fe_t + Mg)$. Diamond = ferrodiorite; circle = fine-grained monzonite; triangle = porphyritic monzonite; inverted triangle = biotite gabbro; and square = monzosyenite. Analyses are recalculated to 100%, anhydrous, with all Fe as FeO. Sybille data are from Fuhrman et al. (1988) and Fountain et al. (1981).

TABLE 2.—*Continued*

Biotite gabbro		Granite	Granitic dikes			
RTM 46	RTM 47	RTM 56	GM 23	RTM 32	GM 15B	RTM 43*
48.09	47.27	77.01	68.40	75.93	75.46	86.07
1.85	2.08	0.16	0.50	0.01	0.80	0.25
18.37	18.08	12.16	15.70	13.34	13.30	5.77
11.42	12.35	1.14	3.21	0.43	0.86	1.37
0.19	0.19	0.02	0.05	0.00	0.03	0.03
6.81	7.06	0.09	0.87	0.03	0.12	0.20
9.05	9.30	0.72	2.45	0.29	0.79	0.52
3.00	3.00	2.77	3.38	3.63	3.26	0.04
0.96	0.41	5.40	4.75	5.90	5.42	4.36
0.30	0.32	0.02	0.15	0.00	0.02	0.05
100.04	100.06	99.49	99.46	99.56	99.34	98.66
CIPW norms based on all Fe as FeO						
0.00	0.00	37.76	22.08	31.21	33.25	66.9
0.00	0.00	0.50	0.90	0.46	0.68	0.16
5.67	2.42	31.91	28.07	34.87	32.03	25.77
25.39	25.39	23.44	28.60	30.72	27.59	0.34
33.83	34.66	3.44	11.17	1.44	3.79	2.25
0.00	0.00	0.00	0.00	0.00	0.00	0.00
7.56	7.80	0.00	0.00	0.00	0.00	0.00
0.64	1.96	2.09	7.33	0.85	1.80	2.66
22.75	23.14	0.00	0.00	0.00	0.00	0.00
3.51	3.95	0.30	0.95	0.02	0.15	0.47
0.70	0.74	0.05	0.35	0.00	0.05	0.12

Feldspars

Plagioclase in the Maloin Ranch pluton becomes more sodic (with considerable overlap) in a sequence that corresponds to the progressive Fe enrichment (Fig. 11). Compositional ranges for anorthositic rocks, biotite gabbro, and ferrodiorite all span An_{50}; nomenclature for biotite gabbro and FDi reflects their average plagioclase compositions. Plagioclases in FMZ, PMZ, MSY, QSY, and granite all have average compositions between An_{20} and An_{35}. Coexisting orthoclase perthites show little systematic variation in Ab and Or (Fig. 11), but An component appears to decrease regularly from about 3% in the FMZ to near 1% in the QSY. Microcline in QSY and granite is lowest in An component, and approaches the Or end-member, except in microcline perthites. Representative compositions of Maloin feldspars are compiled in Table 5.

Unlike the Sybille Monzosyenite, direct evidence for ternary feldspars is lacking in the Maloin Ranch pluton.

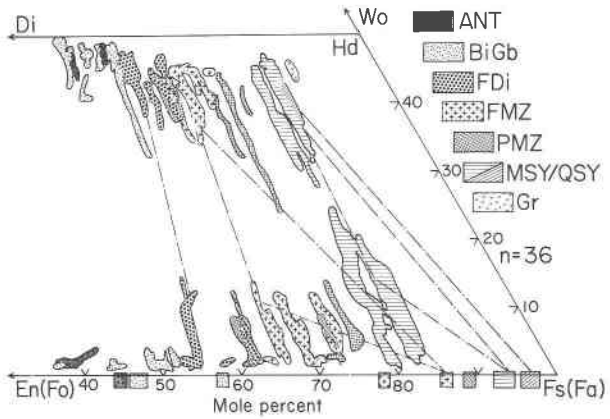

Fig. 9. Compositional variation of pyroxenes (blebs) and olivines (rectangles) in the Maloin Ranch pluton, excluding the layered zone. Tie-lines connect selected coexisting assemblages. Overlap of individual samples is shown only for contrasted rock types. Symbols as in Fig. 2.

TABLE 3. Representative pyroxene analyses

	ANT RTM 11A	FDi RTM 26		FMZ GM 15A		PMZ GM 29C	MSY		QSY RTM 48	Bi Gb RTM 46
	Cpx	Cpx	Opx	Cpx	Pig	Pig	GM 27 Pig	RTM 35 Cpx	Cpx	Cpx
SiO_2	51.66	51.15	50.63	50.39	49.46	48.40	48.01	48.65	48.75	51.96
Al_2O_3	1.93	1.74	0.82	1.25	0.47	0.42	0.32	0.69	0.73	1.87
TiO_2	0.45	0.37	0.13	0.29	0.11	0.12	0.11	0.12	0.21	0.38
FeO(t)*	12.10	14.57	31.53	20.51	38.10	38.70	42.25	28.20	27.57	10.48
MnO	0.34	0.37	0.70	0.41	0.80	0.86	0.91	0.56	0.72	0.29
MgO	11.67	10.38	14.94	8.01	10.13	7.71	5.00	4.35	4.42	12.36
CaO	22.47	21.90	0.87	19.60	0.98	3.94	3.97	17.22	17.81	22.72
Na_2O	0.30	0.29	0.01	0.31	0.02	0.06	0.05	0.28	0.32	0.31
Total	100.92	100.77	99.63	100.77	100.07	100.21	100.62	100.07	100.53	100.37
Cations normalized to 6 oxygens										
Si	1.9421	1.9465	1.9842	1.9612	1.9965	1.9812	1.9916	1.9727	1.9664	1.9497
Al	0.0857	0.0781	0.0380	0.0572	0.0223	0.0201	0.0159	0.0329	0.0348	0.0829
Ti	0.0126	0.0107	0.0039	0.0084	0.0034	0.0035	0.0035	0.0037	0.0062	0.0107
Fe	0.3805	0.4637	1.0335	0.6677	1.2863	1.3249	1.4658	0.9564	0.9298	0.3290
Mn	0.0109	0.0119	0.0234	0.0136	0.0275	0.0297	0.0321	0.0193	0.0246	0.0094
Mg	0.6540	0.5887	0.8727	0.4645	0.6095	0.4703	0.3089	0.2627	0.2658	0.6912
Ca	0.9051	0.8931	0.0367	0.8172	0.0424	0.1726	0.1766	0.7483	0.7697	0.9135
Na	0.0220	0.0211	0.0007	0.0232	0.0013	0.0046	0.0039	0.0219	0.0247	0.0226
Total	4.0129	4.0138	3.9931	4.0130	3.9892	4.0069	3.9983	4.0178	4.0220	4.0090
Wo	46.4	45.6	1.9	41.6	2.2	8.6	8.9	37.7	38.7	47.0
En	33.5	30.1	44.4	23.7	31.0	23.5	15.6	13.2	13.4	35.6
Fs	20.1	24.3	53.8	34.7	66.8	67.8	75.5	49.1	48.0	17.4

* Total Fe as FeO.

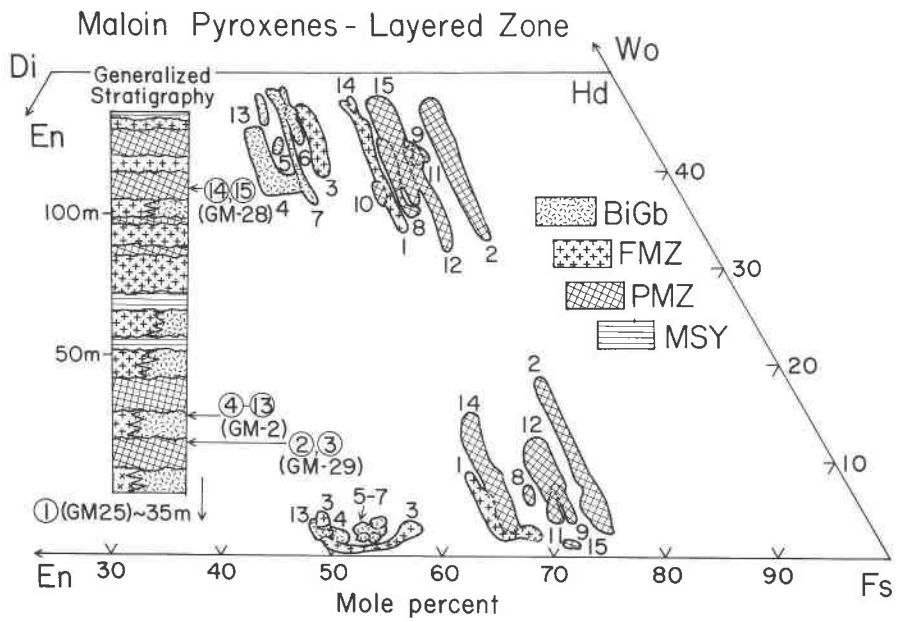

Fig. 10. Compositional variation of pyroxenes in the layered zone. Numbers correspond to relative stratigraphic position, as indicated in accompanying generalized column.

The present two-feldspar assemblages may have originated as ternary compositions, prior to extensive subsolidus re-equilibration. In the Sybille body, exsolved ternary feldspars are present locally in monzogabbro, fine monzonite, and (rarely) monzosyenite (Fuhrman et al., 1988). Most Sybille samples contain only the two-feldspar assemblage observed in the Maloin pluton, with similar compositional trends (Fuhrman et al., Fig. 4). Because inferred temperatures for the Maloin pluton are similar to those for Sybille and to temperatures at which experiments on Sybille samples produced ternary feldspars (Fuhrman, 1986), we suggest that early feldspars in the Maloin Ranch pluton were also ternary. The absence of ternary intergrowths in the Maloin pluton may be attributed to slow cooling, re-equilibration upon intrusion of the Sherman Granite, or for the MSY, influx of volatiles (see Discussion).

TABLE 4. Representative olivine analysis

	FMZ GM 15A	PMZ GM 29C	MSY RTM 35	QSY RTM 48	Bi Gb GM 24
SiO_2	30.67	31.10	30.10	29.70	35.34
Al_2O_3	0.00	—	0.00	0.00	—
TiO_2	0.02	0.02	0.01	0.00	0.02
FeO(t)*	63.34	63.85	66.59	67.78	38.05
MnO	1.05	1.15	1.21	1.42	0.44
MgO	5.11	4.52	2.29	1.15	25.71
CaO	0.03	0.03	0.04	0.02	0.03
Total	100.22	100.67	100.24	100.07	99.59
	Cations normalized to 4 oxygens				
Si	0.9984	1.0082	1.0000	0.9980	1.0007
Al	0.0000	—	0.0000	0.0000	—
Ti	0.0004	0.0004	0.0003	0.0000	0.0006
Fe	1.7242	1.7312	1.8501	1.9049	0.9011
Mn	0.0291	0.0315	0.0342	0.0405	0.0105
Total	3.0009	2.9912	2.9992	3.0018	2.9986
X_{Fe}	0.861	0.873	0.926	0.951	0.451
X_{Mn}	0.015	0.016	0.017	0.020	0.005
X_{Mg}	0.124	0.110	0.057	0.029	0.543
X_{Ca}	0.001	0.001	0.001	0.000	0.000

* Total Fe as FeO.
Note: Dash (—) means not determined.

Fe-Ti oxides

Subequal amounts of ilmenite and titanomagnetite are present in FDi, FMZ, and biotite gabbro, whereas ilmenite is dominant in MSY and QSY. As in Sybille, two generations of ilmenite are common, distinguished by textural relations (e.g., host vs. granules) and by partitioning of Mn (>0.80 wt%) into the secondary ilmenite. Representative analyses of Fe-Ti oxides are given in Table 6.

Hornblende and biotite

Fe-rich hornblendes are present in rocks ranging from monzosyenite to porphyritic granite. In MSY and QSY, hornblende occurs as overgrowths on olivine and pyroxene. Starting with quartz syenite, Fe-rich biotite is also present, in intergrowths with hornblende. In porphyritic granites, hornblende and biotite are the primary ferromagnesian minerals, having compositions similar to late phases in MSY/QSY. Both hornblende and biotite become progressively more Fe enriched with gradation of MSY into porphyritic granite (Fig. 12; Table 7). The Fe-rich hornblendes are similar in composition to hornblende in Proterozoic anorogenic granites (Anderson, 1980, 1983) and in pyroxene ferrosyenite of some alka-

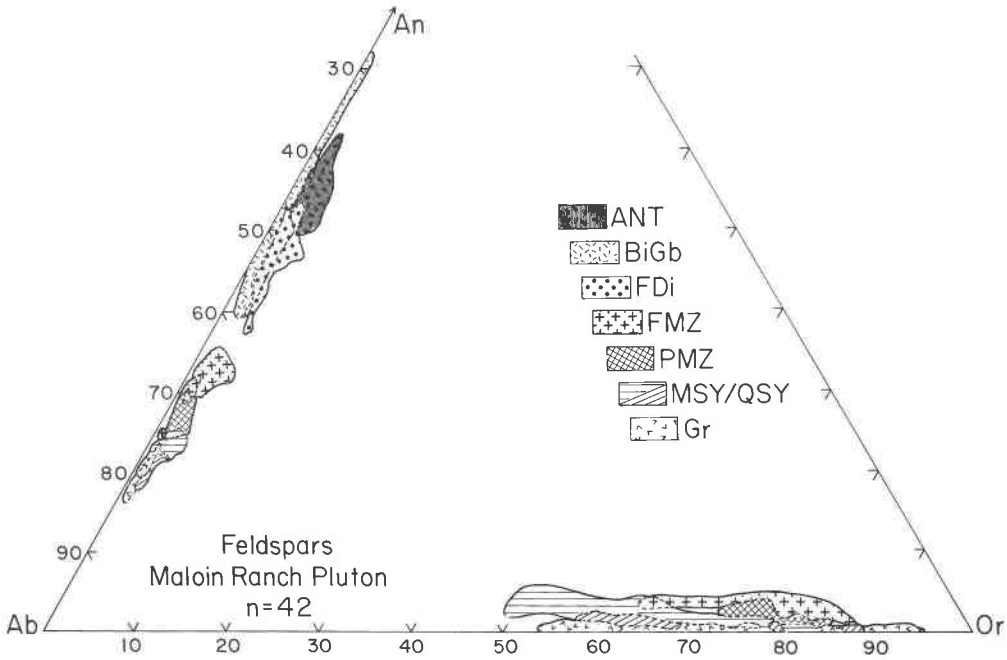

Fig. 11. Compositions of Maloin feldspars (in mol%)

line igneous complexes (Parsons, 1979, 1981; Mitchell and Platt, 1978).

In both hornblendes and biotites, an increase in $^{[4]}$Al appears to accompany the increasing $Fe_t/(Fe_t + Mg)$ ratio (Fig. 12). Calculated A-site occupancy ranges from about 0.4 to 0.65 for average hornblende compositions (formula based on sum of 13 cations, exclusive of Na, K, and Ca; all Fe as FeO). Nomenclature for these amphiboles includes ferrohornblende [$(Na + K)_A < 0.50$], hastingsitic hornblende, and ferro-edenitic hornblende [$(Na + K)_A > 0.50$; Leake, 1978]. Fe favors hornblende over most coexisting biotites (Fig. 12). The most Fe-enriched biotites have the highest $^{[6]}$Al (up to about 0.6 cations/formula). In both hornblende and biotite, Mn content increases progressively from MSY to granite, a typical late-magmatic trend (Table 7).

In biotite gabbro, biotite has intermediate $Fe_t/(Fe_t + Mg)$ ratios, little- or no $^{[6]}$Al, and relatively high Ti (0.5 to 0.7 cations/formula; Table 7). The Ti may help stabilize biotite, which is commonly present with little or no amphibole, in a relatively dry environment.

Geothermometry and geobarometry

Monzonites and monzosyenites in the Laramie Anorthosite Complex contain several assemblages that allow determination of crystallization and subsolidus conditions. For the Sybille Monzosyenite, Fuhrman et al. (1988) found that integrated pyroxene and ternary-feldspar compositions gave the best estimates of primary temperatures. Temperatures above 1000 °C and near 950 °C were inferred for FMZ and MSY, respectively, using the graphical pyroxene thermometer of Lindsley (1983) and the feldspar thermometer of Fuhrman and Lindsley (1988). In the Maloin pluton, integrated augites and pigeonites give minimum temperatures of 900–940 °C for MSY, and a minimum temperature of 970 °C is indicated by a pigeonite from FMZ (Table 8). Pyroxene temperatures obtained using the graphical thermometer (Lindsley, 1983) are similar to those predicted by the pyroxene solution

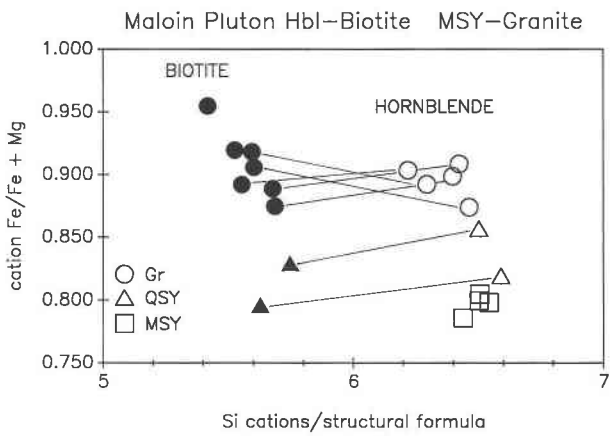

Fig. 12. Fe-enrichment trend in biotite (solid symbols) and hornblende (open symbols) plotted vs. Si cations per formula unit, based on 22 and 23 oxygens, respectively. Fe/(Fe + Mg) is given as the cation fraction. Hornblende formula calculated to sum of 13 cations, exclusive of Na, Ca, and K; all Fe as FeO. Square = monzosyenite; triangle = quartz syenite; circle = porphyritic granite. Tie-lines connect phases in the same sample. Data are averages of multiple analyses.

TABLE 5. Representative feldspar analyses

	ANT RTM 11A	FDi RTM 26	FMZ GM 15A		FMZ GM 25		MSY RTM 35		MSY GM 27	
	Plag	Plag	Plag	Ksp	Plag	Ksp	Plag	Ksp	Plag	Ksp
SiO_2	54.69	55.67	60.74	64.54	59.95	63.88	62.66	65.32	62.10	65.32
Al_2O_3	28.50	27.87	24.74	18.92	24.69	19.11	23.64	18.82	23.86	18.99
TiO_2	0.02	0.04	—	—	0.00	0.02	0.04	0.04	0.03	0.03
FeO(t)*	0.34	0.16	0.21	0.07	0.13	0.06	0.04	0.06	0.08	0.00
CaO	10.87	9.89	6.65	0.48	6.55	0.74	4.75	0.08	5.25	0.32
Na_2O	5.13	5.56	7.77	1.97	7.69	1.99	8.78	2.32	8.62	3.20
K_2O	0.43	0.63	0.16	13.35	0.48	13.45	0.49	13.44	0.35	11.90
BaO	—	—	—	—	—	—	—	—	—	—
Total	99.97	99.82	100.27	99.33	99.49	99.24	100.40	100.08	100.29	99.76
			Cations normalized to 8 oxygens							
Si	2.4707	2.5125	2.6967	2.9753	2.6872	2.9550	2.7673	2.9867	2.7488	2.9804
Al	1.5178	1.4826	1.2953	1.0284	1.3041	1.0419	1.2306	1.0143	1.2449	1.0217
Ti	0.0006	0.0014	—	—	0.0000	0.0006	0.0012	0.0014	0.0009	0.0011
Fe	0.0116	0.0054	0.0078	0.0025	0.0044	0.0020	0.0013	0.0021	0.0027	0.0000
Ca	0.5261	0.4780	0.3165	0.0237	0.3145	0.0365	0.2250	0.0038	0.2489	0.0155
Na	0.4489	0.4869	0.6693	0.1759	0.6681	0.1784	0.7514	0.2058	0.7398	0.2833
K	0.0246	0.0361	0.0092	0.7852	0.0276	0.7935	0.0276	0.7840	0.0196	0.6931
Ba	—	—	—	—	—	—	—	—	—	—
Total	5.0003	5.0030	4.9948	4.9910	5.0059	5.0079	5.0044	4.9981	5.0056	4.9951
Or	2.47	3.60	0.92	79.73	2.73	78.69	2.74	78.90	1.94	69.88
Ab	44.91	48.64	67.27	17.86	66.14	17.70	74.85	20.71	73.37	28.56
An	52.62	47.75	31.81	2.41	31.13	3.62	22.41	0.39	24.69	1.56

Note: Dash (—) means not determined.
* Total Fe as FeO.

model of Davidson and Lindsley (1989) for integrated compositions projected in the pure Fe-Mg-Ca system.

Because ternary feldspar is lacking in the Maloin Ranch pluton, feldspar thermometry only reflects subsolidus conditions in the 600–700 °C range (Table 8). In rocks containing two oxides, ilmenite and titanomagnetite typically occur in coarse, composite intergrowths with varied proportions, making it difficult to reconstruct unexsolved compositions with certainty. Apatite saturation temperatures (Harrison and Watson, 1984) of about 1000 °C are predicted for Maloin FDi and FMZ, fine-grained rocks that probably approximate liquid compositions (Table 8).

TABLE 6. Representative Fe-Ti oxide analyses

	FDi RTM 26		FMZ GM 15A		MSY RTM 35	QSY RTM 48		Bi Gb GM 24	
	Mt	Ilm	Mt	Ilm	Ilm	Ilm-1	Ilm-2	Mt	Ilm
SiO_2	0.07	0.00	0.10	0.03	0.03	0.03	0.03	0.07	0.01
Al_2O_3	2.01	0.00	1.13	0.04	0.02	0.02	0.04	0.87	0.05
TiO_2	5.94	52.14	0.82	50.73	50.16	50.72	51.62	0.38	52.10
FeO	36.90	44.97	32.04	44.71	44.33	44.80	45.20	31.30	45.35
Fe_2O_3*	56.06	1.68	67.62	4.05	5.00	3.71	2.06	66.99	2.29
MnO	0.06	0.58	0.02	0.61	0.60	0.67	1.17	0.03	0.62
MgO	0.20	0.74	0.04	0.17	0.09	0.07	0.01	0.06	0.49
CaO	—	—	0.00	0.00	0.00	0.06	0.01	0.00	0.01
Total	101.24	100.11	100.56	100.34	100.23	100.08	100.14	99.70	100.92
			Cation normalization based on 32 oxygens for Mt and 6 oxygens for Ilm						
Si	0.0205	0.0000	0.0293	0.0013	0.0016	0.0014	0.0014	0.0217	0.0007
Al	0.7085	0.0000	0.4042	0.0021	0.0015	0.0015	0.0024	0.3168	0.0027
Ti	1.3341	1.9681	0.1865	1.9211	1.9031	1.9267	1.9585	0.0867	1.9550
Fe^{2+}	9.2200	1.8875	8.1475	1.8828	1.8707	1.8924	1.9073	8.0430	1.8925
Fe^{3+}	12.6021	0.0635	15.1929	0.1536	0.1899	0.1409	0.0782	15.4875	0.0860
Mn	0.0157	0.0248	0.0053	0.0259	0.0258	0.0288	0.0501	0.0067	0.0264
Mg	0.0879	0.0557	0.0188	0.0124	0.0066	0.0055	0.0011	0.0258	0.0361
Ca	—	—	0.0000	0.0000	0.0000	0.0032	0.0005	0.0000	0.0003
Total	23.9888	3.9996	23.9845	3.9992	3.9992	4.0004	3.9995	23.9882	3.9997
Mt	0.826	—	0.976	—	—	—	—	0.989	—
Usp	0.174	—	0.024	—	—	—	—	0.011	—
Ilm	—	0.983	—	0.961	0.952	0.964	0.980	—	0.978
Hem	—	0.017	—	0.039	0.048	0.036	0.020	—	0.022

* For Mt, $Fe^{3+} = \frac{2}{3}(Fe - Al/2 - 2Ti + Mn + Mg)$; For Ilm, $Fe^{3+} = (Fe - Ti + Mn + Mg)$.

TABLE 5.—*Continued*

QSY RTM 48			Granite RMT 39		Bi Gb GM 24
Plag	Ksp	Mcl	Plag	Mcl	Plag
62.93	65.86	65.38	62.73	65.21	54.15
23.78	18.92	18.72	24.04	18.82	28.46
—	—	—	—	—	0.04
0.07	0.04	0.02	0.09	0.02	0.10
4.65	0.22	0.01	5.01	0.08	10.98
9.16	4.07	1.54	8.87	0.97	5.22
0.29	11.31	14.98	0.31	15.73	0.11
0.00	0.34	0.17	0.07	0.15	—
100.88	100.76	100.82	101.12	100.98	99.06
Cations normalized to 8 oxygens					
2.7655	2.9807	2.9884	2.7534	2.9837	2.4658
1.2318	1.0094	1.0088	1.2436	1.0150	1.5272
—	—	—	—	—	0.0013
0.0023	0.0013	0.0006	0.0029	0.0006	0.0034
0.2188	0.0107	0.0005	0.2356	0.0037	0.5359
0.7809	0.3574	0.8736	0.0173	0.9181	0.0065
0.0163	0.6531	0.1369	0.7552	0.0865	0.4606
0.0000	0.0060	0.0030	0.0012	0.0027	—
5.0156	5.0186	5.0118	5.0092	5.0103	5.0007
1.60	63.96	86.41	1.71	91.06	0.65
76.86	34.99	13.54	74.92	8.58	45.92
21.54	1.05	0.05	23.37	0.37	53.43

Zircon saturation temperatures (Watson and Harrison, 1983) for the same samples are near 750 °C. For Maloin MSY, saturation thermometers give apparent temperatures of 875 to 900 °C, in agreement, within error, with pyroxene thermometry. Because the presence of cumulus feldspar in MSY lowers the calculated temperatures at which apatite and zircon appear, these temperatures must be minima. The magnitude of this effect is not large, as saturation temperatures for MSY show little variation despite large differences in the extent of feldspar accumulation for various samples (Table 8; Kolker, 1989).

Late-magmatic temperatures of 770–850 °C are indicated for MSY, QSY, and porphyritic granite, according to a preliminary temperature calibration of $^{[4]}Al$ content in amphibole (Nabelek and Lindsley, 1985; pers. comm., 1987), at the pressure inferred below (4.3 kbar). Late(?) hornblende in one biotite gabbro (RTM 46) gives a temperature of 900 °C.

Pressure conditions in the Maloin pluton are constrained by the breakdown of Fe-rich pigeonite to fayalitic olivine + quartz + hedenbergite, an equilibrium that is pressure-sensitive (Lindsley and Grover, 1980; Lindsley, 1983). The entire four-phase assemblage—Pig + Fa + Hd + Qtz—is present in some MSY samples (e.g.,

TABLE 7. Representative amphibole and biotite analyses

	Biotite				Hornblende				
	Bi Gb GM 24	Bi Gb RTM 46	QSY RTM 48	Gr RTM 62	Bi Gb RTM 46	MSY RTM 35	QSY RTM 48	Gr RTM 56	Gr RTM 62
SiO_2	37.17	36.99	34.83	34.22	42.00	41.20	42.03	40.85	38.90
Al_2O_3	14.73	14.01	13.37	16.20	12.03	9.75	8.58	8.74	10.50
TiO_2	5.38	5.34	2.17	2.38	3.08	1.78	1.29	0.91	1.51
Cr_2O_3	0.00	0.03	0.03	—	0.02	0.00	0.02	0.00	—
MgO	15.52	13.65	4.59	1.46	11.41	3.59	3.61	2.50	1.43
FeO(t)*	13.60	15.46	32.73	32.26	13.79	28.17	28.99	31.05	30.91
MnO	0.02	0.03	0.10	0.22	0.15	0.21	0.30	0.49	0.59
CaO	0.00	0.00	0.04	0.00	11.14	10.52	10.55	10.24	10.50
Na_2O	0.35	0.24	0.02	0.09	2.14	1.66	1.39	1.87	1.57
K_2O	9.07	9.46	8.59	8.93	1.50	1.34	1.19	1.30	1.76
F	0.32	0.62	0.30	0.17	0.36	0.19	0.16	0.30	0.18
Cl	0.08	0.39	0.03	0.56	0.52	0.27	0.16	0.40	0.74
O≡F,Cl	−0.15	−0.35	−0.14	−0.20	−0.27	−0.14	−0.11	−0.22	−0.25
Total	96.09	95.87	96.66	96.28	97.87	98.54	98.16	98.43	98.34
	Cations per 22 oxygens				**Cations per 23 oxygens**				
Si	5.4838	5.5589	5.6166	5.5446	6.2914	6.5293	6.6903	6.6059	6.3444
Al	2.5615	2.4822	2.5402	3.0930	2.1239	1.8204	1.6094	1.6650	20191
Ti	0.5964	0.6038	0.2632	0.2900	0.3465	0.2121	0.1548	0.1103	0.1852
Cr	0.0000	0.0031	0.0043	—	0.0026	0.0000	0.0024	0.0000	—
Mg	3.4138	3.0575	1.1031	0.3528	2.5467	0.8488	0.8573	0.6030	0.3483
Fe	1.6776	1.9432	4.4142	4.3717	1.7277	3.7344	3.8589	4.1985	4.2167
Mn	0.0023	0.0039	0.0139	0.0299	0.0188	0.0276	0.0409	0.0674	0.0813
Ca	0.0000	0.0000	0.0063	0.0000	1.7880	1.7858	1.7999	1.7744	1.8346
Na	0.0995	0.0695	0.0063	0.0275	0.6201	0.5087	0.4289	0.5849	0.4966
K	1.7075	1.8142	1.7660	1.8460	0.2866	0.2711	0.2414	0.2684	0.3662
Total	15.5424	15.5363	15.7341	15.5555	15.7523	15.7382	15.6842	15.8778	15.8924
F	0.1484	0.2947	0.1545	0.0851	0.1706	0.0967	0.0811	0.1534	0.0949
Cl	0.0198	0.0983	0.0068	0.1530	0.1320	0.0733	0.0442	0.1093	0.2035

Note: Dash (—) means not determined.
* (t) Total Fe as FeO.

TABLE 8. Summary of thermometry and barometry for samples from Maloin Ranch pluton

	Fine-grained monzonite			Monzosyenite					Quartz syenite		Granite
	GM 15A	GM 9	Avg. Syb.*	GM 27	RTM 35	GM 12B	RTM 21A	Avg. Syb.*	RTM 48	RTM 36	RTM 56
Thermometers (°C)											
Pigeonite**	>970	—	>1000	>910	>905	>940	—	—	—	—	—
Clinopyroxene**	>900	—	>1020	—	—	>910	—	—	—	—	—
Two-feldspar†	625	625	600–700	—	650	—	—	600–700	—	—	—
Ternary-feldspar†	—	—	>1050	—	—	—	—	900; >970	—	—	—
Apatite††	1030	1000	1000	890	875	—	—	850–900	—	—	828
Zircon‡	730	770	700–750	890	905	—	—	900	—	—	841
Hornblende‡‡	—	—	—	795	800	820	795	—	770	795	800
Barometers (kbar)											
Pigeonite§	—	—	>2.5	>3.9	>4.0	>4.2	—	—	—	—	—
Olivine§	—	—	<3.0	—	<4.3–5.6	<4.2–5.0	<4.3–5.6	—	<5.3–6.4	<5.9–7.1	—
Hornblende§§	—	—	—	4.4	4.7	4.7	—	—	4.1	4.1	4.8

* Sybille data from Fuhrman et al. (1988).
** Pyroxene thermometry—Lindsley (1983).
† Feldspar thermometry—Fuhrman and Lindsley (1988).
†† Apatite saturation—Harrison and Watson (1984).
‡ Zircon saturation—Watson and Harrison (1983).
‡‡ Amphibole thermometer—Nabelek and Lindsley (1985; pers. comm., 1987).
§ Fe-rich pig. = ol + qtz + hd barometer—Davidson and Lindsley solution model (1989). See text for discussion of the effect of Mn on uncertainty.
§§ Amphibole barometer—Hammarstrom and Zen (1986).

RTM 35; GM12 B) and defines a unique pressure for equilibrium compositions. Pressure is also bracketed by MSY samples containing only pigeonite (giving minimum pressure; e.g., GM 27) and by QSY samples that lack pigeonite but contain Fa + Hd + Qtz (giving maximum pressure; e.g., RTM 48). Using the solution model of Davidson and Lindsley (1989), an average pressure of 4.3 kbar was obtained for rocks with the full assemblage (Table 8), with uncertainties of about 1 kbar (upper) and 0.5 kbar (lower; see below). The model of Davidson and Lindsley offers an improved treatment of forbidden-zone topology compared to that of Lindsley (1983), and the inferred pressure is about 1 kbar lower than that indicated (for the same analyses) by the earlier method. Pressures of ~3 kbar indicated for the Sybille Monzosyenite by Fuhrman (1986) and Fuhrman et al. (1988) using the graphical method may need to be revised correspondingly downward.

A major source of uncertainty in the pressure determinations is the treatment of Mn in expressing pure quadrilateral compositions (X_{Mg} and X_{Ca}) for pyroxenes and olivines, in the Davidson and Lindsley (1989) solution model. For olivines, most microprobe online mineral formulations calculate Fa as (Fe + Mn)/(Fe + Mg + Mn), [=(1 − X_{Mg})]. Expressed in this manner, compositions of olivines from Maloin MSY are nearly 2 mol% more "Fe-rich" than those resulting from adding Mn to Mg, yielding Fo as (1 − X_{Fe}). This difference gives a range of about 1 kbar for pressure maxima, with compositions expressed as (1 − X_{Fe}) giving the minimum upper bracket (Table 8). For pigeonites, an analogous range in minimum pressures of about 0.5 kbar results from uncertainty in expressing X_{En}. The presence of Mn may also extend the stability of Fe-rich pyroxenes to lower pressures. Bohlen et al. (1980) found that each mole percent $MnSiO_3$ added to ferrosilite extended its stability by about 0.12 kbar, relative to pure $FeSiO_3$, in the equilibrium ferrosilite = fayalite + quartz.

Pressures indicated by Al content of amphibole (Hammerstrom and Zen, 1986) range from 4.1 to 4.8 kbar, in good agreement with pressures given by the assemblage Pig + Fa + Hd + Qtz, for samples that allow both estimates (Table 8).

Oxygen fugacity

Because of extensive subsolidus re-equilibration, conventional Fe-Ti oxide thermobarometry cannot be used with certainty to obtain estimates of primary temperatures and f_{O_2} in the Maloin Ranch pluton. In the MSY and QSY, Fe-Ti oxides (primarily ilmenite) coexist with fayalitic olivine and quartz, an assemblage controlled by the equilibrium quartz + ulvöspinel = ilmenite + fayalite (QUIIF; Frost et al., 1988a). In the full QUIIF assemblage, temperature and f_{O_2} are overdetermined, allowing primary T-f_{O_2} conditions to be estimated even if the Fe-Ti oxides have re-equilibrated, provided that pressure is known within 1–2 kbar (Frost et al., 1988a). To do so, we use the intersections of the QUIIF surface (displaced for X_{Mg} in fayalite) with ilmenite isopleths of the Fe-Ti oxide geothermometer (Andersen and Lindsley, 1988), as shown in Figure 13. These intersections give maximum T and minimum f_{O_2} of equilibration (see Frost et al., 1988a, method 2); for ilmenite-dominated oxide assemblages such as the MSY and QSY, these values are very close to the actual T and f_{O_2}. This method indicates a primary temperature range of ~950–1000 °C for the MSY and QSY, with f_{O_2} ranging from 1 to 2 log units below the FMQ buffer (Fig. 13). Oxygen fugacity can also be

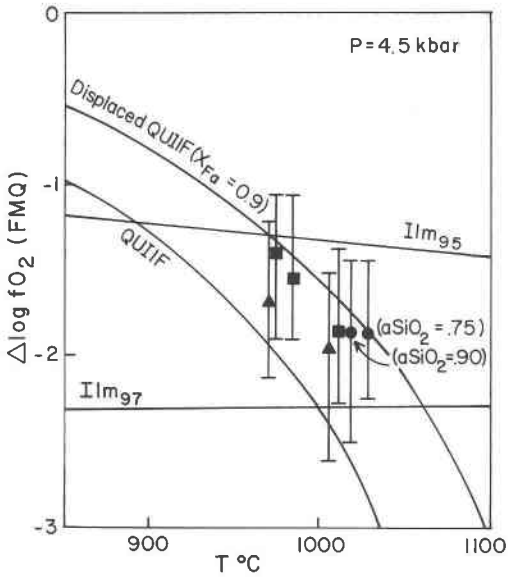

Fig. 13. Temperature vs. $\Delta\log f_{O_2}$ (FMQ) [$(\log f_{O_2})_{sample} - (\log f_{O_2})_{FMQ}$] plot showing intersections of Ilm_{95} and Ilm_{97} isopleths with QUIIF surface displaced for $X_{Fa} < 1.0$. High-temperature intersection suggests primary oxides equilibrated at ~950–1025 °C. A primary f_{O_2} of 1–2 log units below FMQ is inferred from intersections. Error bars show range in f_{O_2} resulting from 1% error in ilmenite analyses. Square = monzosyenite; triangle = quartz syenite; circle = fine monzonite.

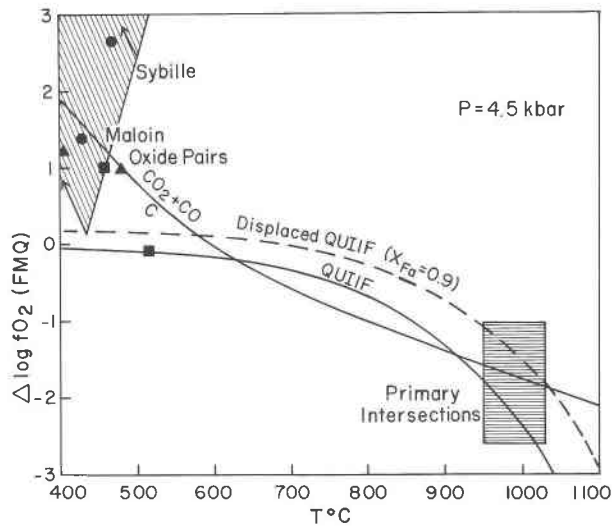

Fig. 14. Temperature vs. $\Delta\log f_{O_2}$ plot showing field of inferred primary conditions (from Fig. 13; shown by horizontally striped field) and subsolidus conditions indicated by oxide pairs in the same samples. The oxide pairs suggest an early cooling path along displaced QUIIF, followed by late graphite saturation, as in the Sybille Monzosyenite, shown by diagonally striped field. Low-temperature T-f_{O_2} relations extrapolated from the Andersen and Lindsley (1988) Fe-Ti oxide geothermometer.

estimated for the FMZ (which lacks quartz), by varying silica activity until displaced QUIIF intersects the appropriate primary temperature as estimated from other geothermometers. For two FMZ samples, this gives an f_{O_2} of about 1.75 log units below FMQ, using silica activities of 0.75 (RTM 20) and 0.9 (GM 15A). The reducing primary conditions estimated for the Maloin Ranch pluton agree with f_{O_2} determinations for the Sybille Monzosyenite (Fuhrman et al., 1988).

Although most samples of MSY and QSY are ilmenite-dominated, the presence of isolated magnetite-ilmenite sandwich grains having Usp-rich integrated compositions confirms that two oxides (and therefore the full QUIIF assemblage) were present at high temperature. These isolated magnetite-ilmenite grains are rarely in contact with fayalite, and the dominant assemblage Fa + Ilm + Qtz suggests a cooling path at or below displaced QUIIF (Fig. 14). Present Fe-Ti oxide compositions record final equilibration near or below 500 °C, at average f_{O_2} conditions ~1 log unit above FMQ. The f_{O_2} is slightly more reducing than that found by Fuhrman et al. (1988) for low-temperature oxide pairs in the Sybille Monzosyenite. Fuhrman et al. have shown that Sybille cooled in the presence of CO_2-rich fluid, with f_{O_2} upon cooling controlled by equilibria involving graphite, not by QUIIF. For the Maloin pluton, the array of low-temperature oxide pairs suggests a cooling f_{O_2} path that was probably controlled by displaced QUIIF early, followed by late graphite saturation (Fig. 14). The presence of graphite in the Maloin MSY (as inclusions in feldspar) has recently been determined (J. Touret, pers. comm., 1988).

Water fugacity

Additional information on fluid fugacities can be obtained by using the equilibrium annite + quartz = K-feldspar + fayalite (+ H_2O) for Maloin quartz syenites (samples RTM 48, RTM 36). Water fugacity appears to have been moderate in QSY. This estimate is limited primarily by uncertainties in expressing annite activity in biotite and in temperature. We selected temperatures between 700 and 800 °C for the calculation because amphibole coexisting with biotite in both samples gives temperatures near 800 °C (Table 8). Activity models for annite include multisite ($X_K X^3_{[6]Fe} X^3_{Si} X^2_{OH}$) and simple ($X^3_{[6]Fe}$) ionic models. Minimum values of a_{Annite} and f_{H_2O} are given by the multisite model. Using this model, f_{H_2O} for 750 °C is estimated to be about 1700 bars (P_{total} = 4.5 kbar). At the same temperature, f_{H_2O} estimated using the simple ionic model for annite activity is 2100–2300 bars. At 800 °C, estimated f_{H_2O} bracketed by the two annite activity models is increased to 2300–3100 bars. The K-feldspar activity used in the equilibrium calculations was determined with the ternary-solution model of Fuhrman and Lindsley (1988). Activity of fayalite in olivine was calculated as X^2_{Fe}.

Discussion

In its lithologic succession and bulk chemistry, the Maloin Ranch pluton is like many intermediate to felsic in-

trusions surrounding massif anorthosites and like parts of some alkalic igneous bodies. These intrusions were typically emplaced under hot, dry conditions, as indicated by the presence of ternary mesoperthites (e.g., Parsons, 1981; Wiebe and Wild, 1983). In the Sybille Monzosyenite, ternary feldspar is widely scattered in monzogabbro, fine monzonite, and rarely, in monzosyenite (Fuhrman et al., 1988). The similarity of the Maloin pluton to intrusions containing ternary feldspar is such that we strongly suspect it to have been a primary phase. Pyroxene and saturation thermometers indicate that appropriate temperatures existed (~1000 °C), but feldspar pairs reflect re-equilibration at 600–700 °C.

The breakdown of Maloin ternary feldspars and other subsolidus events appear to be a consequence of several factors. For monzosyenites, Maloin may have contained more H_2O than Sybille, as late hornblende is much more abundant. Perhaps more significant is the location of the Maloin pluton between two much larger intrusive bodies. Heat from the Laramie Anorthosite and Sherman Granite probably slowed cooling in the Maloin pluton, and considerable re-equilibration may have accompanied emplacement of the granite. Thus, textural evidence for ternary feldspars is now lacking, even in chilled FMZ from the layered zone. In comparison, the Sybille Monzosyenite is bounded to the north by Archean country rocks and so may have cooled more rapidly. The greater depth of emplacement of the Maloin Ranch pluton would also contribute to slower cooling.

On the basis of geologic mapping, mineral chemistry, and crystallization experiments, Fuhrman et al. (1988) have suggested that all rock types in the Sybille Monzosyenite (monzogabbro to monzosyenite) are probably part of a single differentiation sequence, although they recognized that some mixing may have also occurred. Petrologic data for the Maloin pluton present some further restrictions. As recognized by Fuhrman et al., the relative volumes of exposed rock types are inconsistent with in situ fractionation of a single magma, and a magma chamber at depth would be required to produce the entire series. The observed range in Fe enrichment and the enrichment in incompatible elements (Kolker and Lindsley, 1986a; Kolker, 1989) would require very large extents of fractionation, if all rock types are members of a single closed series. For example, >90% fractionation of the FDi would be required to produce the Rb concentration in the average FMZ. Intrusive relations in the Maloin pluton show that different parts of the series coexisted as magmas, requiring fractionation of multiple batches of magma if all members are related by similar liquid lines of descent.

Forming the FMZ to MSY series by mixing could allow the range in rock types and mineral compositions to be produced in place. Mixing of FMZ and MSY in the Maloin pluton has produced some PMZ, but it is not certain that Sybille PMZ formed by this process. Hybridization of FMZ and MSY would be facilitated by their similar bulk compositions and emplacement temperatures (e.g., Frost and Mahood, 1987). Distinguishing well-homogenized hybrids can be difficult where petrographic evidence for mixing is lacking (e.g., Dungan, 1987). Textural evidence for mixing of FMZ and MSY in the Maloin pluton is sufficiently strong to consider mixing as an alternative to a continuous fractionation series in that body, possibly requiring separate origins for FMZ and MSY, as also suggested by isotopic data (Kolker, 1989).

For the Maloin FMZ, dry mineral assemblages, lack of pelitic inclusions, and isotopic compositions of Sr (Subbarayudu, 1975; Kolker et al., 1988) and Nd (Kolker et al., 1987) suggest no interraction with country rock or high-level granitic melt. However, it is likely that open-system processes accompanied late-magmatic differentiation in the Maloin Ranch pluton. Inclusions of various supracrustal rocks are widespread in Maloin porphyritic granites, and evidence for anatexis of map-scale inclusions was observed at several locations. Open-system behavior is also indicated locally for portions of the Sybille Monzosyenite on the basis of field relations (Fuhrman et al., 1988), Sr-isotope data, and trace-element variation (Subbarayudu, 1975; Fountain et al., 1981). The MSY to granite trends in mineral chemistry probably resulted from some combination of fractionation of MSY and mixing of granitic melt, some of which may have been generated at or near the level of emplacement.

The relation of the FDi to MSY portion of the Maloin Ranch pluton to the Laramie Anorthosite is uncertain. The ferrodiorite appears most likely to be comagmatic with the anorthosite, based on its proximity to the contact and oxide-apatite–rich composition. Although textures of FDi and FMZ suggest that these rock types approximate liquid compositions, REE data do not show substantial negative Eu anomalies complementary to plagioclase cumulates (Kolker and Lindsley, 1986b; Kolker, 1989). Suppression of a strongly negative Eu anomaly in late liquids of the anorthositic series may be due to cotectic crystallization of plagioclase and augite or, in latest stages, by removal of apatite, as shown by Morse and Nolan (1985) for the Kiglapait intrusion. The presence of an initial positive Eu anomaly would have a similar effect, as projected for Kiglapait and observed in fine-grained anorthositic dikes of the Nain Complex (Wiebe, 1980b).

Summary and conclusions

The Maloin Ranch pluton was emplaced into anorthositic rocks at high temperature (up to ~1000 °C for the FDi and FMZ), moderate pressure (4.0–4.5 kbar), and low f_{O_2} (1–2 log units below FMQ at primary temperatures). Nearly continuous trends in the composition of pyroxenes and feldspars are present from FDi to MSY. At the top of the Maloin pluton, the Fe-enrichment trend continues from MSY to porphyritic granite, as shown by the compositions of hornblende and biotite. For Maloin PMZ, the range in mineral chemistry is not the result of a continuous fractionation series, but rather, formed by mixing of FMZ and MSY.

The Maloin Ranch pluton differs from Sybille in the following respects: (1) presence of a well-defined stratigraphy, (2) presence of a layered zone, (3) evidence for the origin of PMZ by mixing of FMZ and MSY, (4) upward gradation of Maloin MSY into surrounding porphyritic granites (occurs only locally at Sybille), (5) lower Fe/(Fe + Mg) in Maloin for similar rock types, (6) absence of ternary feldspars, and (7) higher total pressure (4–4.5 kbar vs. <3 kbar). Despite these differences, similarities in rock types, bulk composition, phase chemistry, and location (at the anorthosite margin), strongly suggest a broadly common history for Maloin and Sybille. Both intrusions probably evolved by similar processes, although detailed histories differed for each intrusion.

Acknowledgments

We thank Carl Anderson, B. R. Frost, Chris Hadjigeorgiou, Tom Hulsebosch, John Kling, Jean Nealon, Steve Tasi, and the late Matthew Valenti for assisting in mapping and sampling. We are grateful to ranchers Pete Burns, Howard Carroll, Charles and Merrill Farthing, and Jim Tugman for allowing access to their land and to Grandma Josephine Burns for uncommon hospitality. P. M. Davidson, B. R. Frost, M. L. Fuhrman, J. A. Grant, G. N. Hanson, S. A. Morse, and R. A. Wiebe contributed much by discussion. Initial reviews by B. R. Frost and W. D. Sharp helped improve the manuscript, as did subsequent reviews by R. F. Emslie and A. R. Philpotts. This study was supported by NSF grant EAR-8618480 to D. H. Lindsley and EAR-8617812 to B. R. Frost and C. D. Frost.

References cited

Aleinikoff, J.N. (1983) U-Th-Pb systematics of zircon inclusions in rock-forming minerals: A study of armoring against isotopic loss using the Sherman Granite of Colorado-Wyoming, USA. Contributions to Mineralogy and Petrology, 83, 259–269.

Andersen, D.J., and Lindsley, D.H. (1988) Internally consistent solution models for Fe-Mg-Mn-Ti oxides: Fe-Ti oxides. American Mineralogist, 73, 714–726.

Anderson, J.L. (1980) Mineral equilibria and crystallization conditions in the late Precambrian Wolf River rapakivi massif, Wisconsin. American Journal of Science, 280, 289–332.

——— (1983) Proterozoic anorogenic plutonism of North America. In L.G. Medaris, Jr., and others, Eds., Proterozoic geology: Selected papers from an international Proterozoic symposium. Geological Society of America Memoir 161, 133–154.

Ashwal, L.D. (1982) Mineralogy of mafic and Fe-Ti oxide-rich differentiates of the Marcy anorthosite massif, Adirondacks, New York. American Mineralogist, 67, 14–27.

Ashwal, L.D., and Siefert, K.E. (1980) Rare-earth element geochemistry of anorthosite and related rocks from the Adirondacks, New York, and other massif-type complexes. Geological Society of America Bulletin, 91, 2, 659–684.

Bence, A.E., and Albee, A.L. (1968) Empirical correction factors for the electron microanalysis of silicates and oxides. Journal of Geology, 76, 382–403.

Bohlen, S.R., Boettcher, A.L., Dollase, W.A., and Essene, E.J. (1980) The effect of manganese on olivine-quartz-orthopyroxene stability. Earth and Planetary Science Letters, 47, 11–20.

Buddington, A.F. (1972) Differentiation trends and parental magmas for anorthositic and quartz mangerite series, Adirondacks, New York. Geological Society of America Memoir 132, 477–488.

Davidson, P.M., and Lindsley, D.H. (1989) Thermodynamic analysis of pyroxene-olivine-quartz equilibria in the system CaO-MgO-FeO-SiO_2. American Mineralogist, 74, 18–30.

Duchesne, J.-C. (1984) Massif anorthosites: Another partisan review. In W.L. Brown, Ed., Felspars and feldspathoids, p. 411–433. D. Reidel, Dordrecht, the Netherlands.

Duchesne, J.-C., Maquil, R., and Demaiffe, D. (1985a) The Rogaland anorthosites: Facts and speculations. In A.C. Tobi, and J.L.R. Touret, Eds., The deep Proterozoic crust in the North Atlantic provinces, p. 449–476. D. Reidel, Dordrecht, the Netherlands.

Duchesne, J.-C., Roelandts, I., Demaiffe, D., and Weis, D. (1985b) Petrogenesis of monzonoritic dykes in the Egersund-Ogna anorthosite (Rogaland, S. W. Norway): Trace elements and isotopic (Sr, Pb) constraints. Contributions to Mineralogy and Petrology, 90, 214–225.

Duebendorfer, E.M., and Houston, R.S. (1987) Proterozoic accretionary tectonics of the southern margin of the Archean Wyoming craton. Geological Society of America Bulletin, 98, 554–568.

Dungan, M.A. (1987) Open system magmatic evolution of the Taos Plateau volcanic field, northern New Mexico: II. The genesis of cryptic hybrids. Journal of Petrology, 28, 955–977.

Emslie, R.F. (1980) Geology and petrology of the Harp Lake Complex, central Labrador: An example of Elsonian magmatism. Geological Survey of Canada Bulletin 293, 136 p.

——— (1985) Proterozoic anorthosite massifs. In A.C. Tobi and J.L.R. Touret, Eds., The deep Proterozoic crust in the North Atlantic provinces, p. 39–60. D. Reidel, Dordrecht, the Netherlands.

Fountain, J.C., Hodge, D., and Hills, F.A. (1981) Geochemistry and petrogenesis of the Laramie Anorthosite Complex. Lithos, 14, 113–132.

Fowler, K.S. (1930) The anorthositic area of the Laramie Mountains, Wyoming. American Journal of Science, 219, 373–405.

Frost, T.P., and Mahood G.A. (1987) Field, chemical, and physical constraints on mafic-felsic magma interaction in the Lamark Granodiorite, Sierra Nevada, California. Geological Society of America Bulletin, 99, 272–291.

Frost, B.R., Lindsley, D.H., and Andersen, D.J. (1988a) Fe-Ti oxide-silicate equilibria: Assemblages with fayalitic olivine. American Mineralogist, 73, 727–740.

Frost, C.D., Meier, M., Oberli, F., and Manning, L.D. (1988b) Single crystal U-Pb zircon study of the Red Mountain pluton, Laramie Anorthosite Complex, Wyoming (abs.). EOS, 69, 520.

Fuhrman, M.L. (1986) The petrology and mineral chemistry of the Sybille Monzosyenite and the role of ternary feldspars. Ph.D. thesis, 214 p. State University of New York, Stony Brook, New York.

Fuhrman, M.L., and Lindsley, D.H. (1988) Ternary feldspar modeling and thermometry. American Mineralogist, 73, 201–215.

Furhman, M.L., Frost, B.R., and Lindsley, D.H. (1988) Crystallization conditions of the Sybille Monzosyenite, Laramie Anorthosite Complex, Wyoming. Journal of Petrology, 29, 699–729.

Geist, D.J., Frost, C.D., and Frost, B.R. (1987) Delineation of a hidden Archean-Proterozoic suture: Nd isotopes in the Sherman Granite. Geological Society of America Abstracts with Programs, 19, 674.

Harrison, T.M., and Watson, E.B. (1984) The behavior of apatite during crustal anatexis: Equilibrium and kinetic considerations. Geochimica et Cosmochimica Acta, 48, 1467–1477.

Hammarstrom, J.M., and Zen, E-an, (1986) Aluminum in hornblende: An empirical igneous geobarometer. American Mineralogist, 71, 1297–1313.

Hills, F.A., and Armstrong, R.L. (1974) Geochronology of Precambrian rocks in the Laramie Range and implications for the tectonic framework of Precambrian southern Wyoming. Precambrian Research, 1, 213–225.

Karlstrom, K.E., and Houston, R.S. (1984) The Cheyenne Belt: Analysis of a Proterozoic suture in southern Wyoming. Precambrian Research, 25, 415–446.

Klugman, M.A. (1966) Resume of the geology of the Laramie Anorthosite mass. Mountain Geologist, 3, 75–84.

Kolker, Allan. (1989) Petrology and geochemical evolution of the Maloin Ranch pluton, Laramie Anorthosite Complex, Wyoming. Ph.D. thesis, State University of New York, Stony Brook, New York.

Kolker, Allan, and Lindsley, D.H. (1986a) Geochemistry of monzonites and monzosyenites in the Maloin Ranch pluton, Laramie Anorthosite Complex, Wyoming. Geological Society of America Abstracts with Programs, 18, 660.

——— (1986b) Field petrology and REE geochemistry of the Maloin Ranch pluton, Laramie Anorthosite Complex, Wyoming (abs.). EOS, 67, 385.

Kolker, Allan, Lindsley, D.H., and Hanson, G.N. (1987) Implications of Nd isotopes in the Maloin Ranch pluton, Laramie Anorthosite Complex (LAC), Wyoming (abs.). EOS, 68, 430.

Kolker, Allan, Lindsley, D.H., and Geist, D.J. (1988) Fractionation(?), mixing, and assimilation in the Maloin Ranch pluton, Laramie Anorthosite Complex, Wyoming (abs.). EOS, 69, 513.

Leake, B.E. (1978) Nomenclature of amphiboles. American Mineralogist, 63, 1023–1052.

Lindsley, D.H. (1983) Pyroxene thermometry. American Mineralogist, 68, 477–493.

Lindsley, D.H., and Grover, J.E. (1980) Fe-rich pigeonite: A geobarometer. Geological Society of America Abstracts with Programs, 12, 472.

Lindsley, D.H., Fuhrman, M.L., and Frost, B.R. (1985) Problems in classification of felsic plutonic rocks containing ternary feldspars (abs.). EOS, 66, 416.

Livi, K.J.T. (1987) Geothermometry of exsolved augites from the Laramie Anorthosite Complex, Wyoming. Contributions to Mineralogy and Petrology, 96, 371–380.

Mitchell, R.H., and Platt, R.G. (1978) Mafic mineralogy of ferroaugite syenite from the Coldwell alkaline complex, Ontario, Canada. Journal of Petrology, 19, 627–651.

Morse, S.A. (1982) A partisan review of Proterozoic anorthosites. American Mineralogist, 67, 1087–1100.

Morse, S.A., and Nolan, K.M. (1985) Kiglapait geochemistry VII: Yttrium and the rare earth elements. Geochimica et Cosmochimica Acta, 49, 1621–1644.

Nabelek, C.R., and Lindsley, D.H. (1985) Tetrahedral Al in amphibole: A potential thermometer for some mafic rocks. Geological Society of America Abstracts with Programs, 17, 673.

Newhouse, W.H., and Hagner, A.F. (1957) Geologic map of anorthosite areas, southern part of the Laramie Range, Wyoming. U.S. Geological Survey Mineral Investigations Field Studies Map MF-119.

Norrish, K., and Hutton, J.T. (1969) An accurate X-ray spectrographic method for the analysis of a wide range of geological samples. Geochimica et Cosmochimica Acta, 33, 431–453.

Parsons, Ian. (1979) The Klokken gabbro-syenite complex, south Greenland: Cryptic variation and the origin of inversely graded layering. Journal of Petrology, 20, 653–694.

———(1981) The Klokken gabbro-syenite complex, South Greenland: Quantitative interpretation of mineral chemistry. Journal of Petrology, 22, 233–260.

Parsons, Ian, and Brown, W.L. (1984) Feldspars and the thermal history of igneous rocks. In W.L. Brown, Ed., Feldspars and feldspathoids, p. 317–371. D. Reidel, Dordrecht, the Netherlands.

Petersen, J.S. (1980) The zoned Kleivan granite—An end member of the anorthosite suite in southwest Norway. Lithos, 13, 79–95.

Philpotts, A.R. (1966) Origin of the anorthosite-mangerite rocks in southern Quebec. Journal of Petrology, 7, 1–64.

———(1981) A model for the generation of massif-type anorthosites. Canadian Mineralogist, 19, 233–253.

Snyder, G.L. (1984) Preliminary geologic maps of the central Laramie Mountains, Albany and Platte Counties, Wyoming. U.S. Geological Survey Open-File Report 84-358.

Subbarayudu, G.V. (1975) The Rb-Sr isotopic composition and origin of the Laramie anorthosite-mangerite complex, Laramie Range, Wyoming: Ph.D. thesis, 109 p. State University of New York at Buffalo, New York.

Subbarayudu, G.V., Hills, F.A., and Zartman, R.E. (1975) Age and Sr isotopic evidence for the origin of the Laramie anorthosite-syenite complex, Laramie Range, Wyoming. Geological Society of America Abstracts with Programs, 7, 1287.

Watson, E.B., and Harrison, T.M. (1983) Zircon saturation revisited: Temperature and composition effects in a variety of crustal magma types. Earth and Planetary Science Letters, 64, 295–304.

Wheeler, E.P., II. (1969 [1970]) Minor intrusives associated with the Nain anorthosite. In Y.V. Isachsen, Ed., The origin of anorthosite and related rocks. New York State Museum and Science Service Memoir 18, 189–206.

Wiebe, R.A. (1974a) Coexisting intermediate and basic magmas, Ingonish, Cape Breton Island. Journal of Geology, 82, 74–87.

———(1974b) Differentiation in layered diorite intrusions, Ingonish, Nova Scotia. Journal of Geology, 82, 731–750.

———(1980a) Commingling of contrasted magmas in the plutonic environment: Examples from the Nain anorthosite complex. Journal of Geology, 88, 197–209.

———(1980b) Anorthositic magmas and the origin of Proterozoic anorthosite massifs. Nature, 286, 564–567.

Wiebe, R.A., and Wild, T. (1983) Fractional crystallization and magma mixing in the Tigalak layered intrusion, the Nain anorthosite complex, Labrador. Contributions to Mineralogy and Petrology, 84, 327–344.

Manuscript received June 6, 1988
Manuscript accepted November 25, 1988